Uncovering striatal dopamine synaptogenesis using intersectional genetics in a mouse model of autism spectrum disorder

Sarah Alexandra Martin, B.Sc. (M.Sc. Candidate)

Integrated Program in Neuroscience

McGill University, Montreal

June 2023

A thesis submitted to McGill University in partial fulfillment of the requirements of the degree of Master of Science (M.Sc.) in Neuroscience

Table of Contents

Abstract (English)

Autism Spectrum disorder (ASD) is a neurodevelopmental condition which is heterogenous in both genetic etiology and clinical presentation, which affects approximately 1 in 100 children worldwide. However, the neural basis of ASD remains unknown. Despite the diversity of symptoms, there are two core clinical features (social communication deficits and repetitive behaviours) which are commonly exhibited across the spectrum. Both of these behaviours overlap with functions of the striatum, which is the major input structure of the basal ganglia and receives excitatory glutamatergic input and modulatory dopaminergic (DAergic) input. Dopamine (DA) circuit dysregulation is hypothesized to play a role in the behavioural symptoms of ASD, and current evidence from genetic animal models and human neuroimaging studies supports this hypothesis. Interestingly, research has also shown that neuronal processes during development, such as synapse assembly and synaptic transmission, are disrupted in ASD. Additionally, DA synaptogenesis in normal development is currently poorly understood. Altogether, these insights highlight the importance of understanding how DA circuits develop and how this development is altered in ASD. The goal of this thesis is to uncover DA circuit development using intersectional genetics, and to investigate how DA circuit development may be altered in SHANK3b mutant mice, which is a mouse model of ASD. SHANK3b are expected to show a deficit in social behaviour, which was demonstrated in this thesis using a modified 3-chamber sociability test. To study circuit development, RC::FPSiT mice are crossed with mice that express Cre and Flp recombinases in midbrain DAergic neurons specifically, which results in the expression of synaptophysin GFP (Syn-GFP) at the release sites of neurotransmitters on these neurons. Putative DA release sites in the striatum can thus be visualized in the developing striatum using immunohistochemistry and confocal microscopy. The striatum at specific timepoints (P0, P14,

P21) has been stained and imaged for comparative analysis in normal development. In SHANK3b mutant mice, fluorescence intensity analysis of DAergic and glutamatergic release sites has been conducted for timepoints P0 and P14. The results show that release sites on the projections of midbrain DAergic neurons in the striatum arrange in a patch-and-matrix pattern in early development (P0), which becomes more diffuse by P14 and almost completely diffuse by P21. From P0 to P14, DAergic innervation of the striatum spreads ventrolaterally to dorsomedially, and the nucleus accumbens (NAc) becomes more clearly defined by DAergic innervation by P14. In SHANK3b mutant mice, no significant differences were found in fluorescence intensity of DAergic or glutamatergic projections in the striatum compared to control mice. In conclusion, there does not appear to be a significant difference in the structural aspect of striatal DAergic circuit development in SHANK3b mutant mice, but these results do not give information about possible alterations to DAergic activity in SHANK3b mutant mice, which is the future direction of this research.

Abstract (French)

Le trouble du spectre de l'autisme (TSA) est une affection neurodéveloppementale hétérogène, à la fois en termes d'étiologie génétique et de présentation clinique, qui touche environ 1 enfant sur 100 dans le monde. Cependant, la base neurale des TSA reste inconnue. Malgré la diversité des symptômes, il existe deux caractéristiques cliniques fondamentales (déficits de communication sociale et comportements répétitifs) qui sont couramment présentées dans tout le spectre. Ces deux comportements se chevauchent avec les fonctions du striatum, qui est la principale structure d'entrée des ganglions de la base et reçoit une innervation glutamatergique excitatrice et dopaminergique modulatrice (DAergique). On suppose que la dysrégulation du circuit de la dopamine (DA) joue un rôle dans les symptômes comportementaux des TSA, et les preuves actuelles provenant de modèles animaux transgéniques et d'études de neuro-imagerie humaine soutiennent cette hypothèse. Fait intéressant, la recherche a également montré que les processus neuronaux au cours du développement, tels que l'assemblage des synapses et la transmission synaptique, sont perturbés dans les TSA. De plus, la synaptogenèse de la DA dans le développement normal n'est pas complètement caractérisée. Dans l'ensemble, ces informations soulignent l'importance de comprendre le développement des circuits DAergiques et si celui-ci est affecté dans les TSA. Le but de cette thèse est de découvrir le développement du circuit DA en utilisant la génétique intersectionnelle, et d'étudier comment le développement du circuit DA peut être modifié chez les souris mutantes SHANK3b, qui est un modèle murin de TSA. On s'attend à ce que SHANK3b présente un déficit de comportement social, ce qui a été démontré dans cette thèse à l'aide d'un test de sociabilité modifié à 3 chambres. Pour étudier le développement des circuits, les souris RC::FPSiT sont croisées avec des souris qui expriment les recombinases Cre et Flp dans les neurones DAergiques du mésencéphale spécifiquement, ce qui entraîne l'expression

de la synaptophysine GFP (Syn-GFP) aux sites de libération des neurotransmetteurs sur ces neurones. Les sites putatifs de libération de DA dans le striatum peuvent ainsi être visualisés dans le striatum en développement à l'aide de l'immunohistochimie et de la microscopie confocale pour quatre âge précise (P0, P14, P21). Chez les souris mutantes SHANK3b, une analyse de l'intensité de fluorescence des sites de libération DAergique et glutamatergique a été menée pour les points temporels P0 et P14. Les résultats montrent que les sites de libération DAergiques dans le striatum innervent principalement le striosomeau début du développement postnatal (P0), puis innerve la matrice vers P14 et couvre presque complètement le striatum par P21. De P0 à P14, l'innervation DAergique du striatum se propage ventrolatéralement à dorsomédialement, et le noyau accumbens (NAc) devient plus clairement défini par l'innervation DAergique par P14. Chez les souris mutantes SHANK3b, aucune différence significative n'a été observée dans l'intensité de fluorescence des projections DAergiques ou glutamatergiques dans le striatum par rapport aux souris témoins. En conclusion, il ne semble pas y avoir de différence significative dans l'aspect structurel du développement du circuit DAergique striatal chez les souris mutantes SHANK3b, mais ces résultats ne donnent pas d'informations sur les altérations possibles de l'activité DAergique chez les souris mutantes SHANK3b, ce qui est l'orientation future de cette recherche.

Acknowledgements

Thank you to Dr. Jean-Francois Poulin for your unwavering support throughout this project. You are a dedicated researcher whose excitement about scientific discovery is contagious. Thank you for always pushing me to reach my fullest potential. Your mentorship over these past 3 years is invaluable and has shaped me into a better researcher.

Thank you to my committee members Dr. Yang Zhou and Dr. Jean-Francois Cloutier for your support, and to Dr. Philippe Seguela for kindly sharing your lab space with us.

A big thank you to Lucia Guerra for assisting with data collection for this project, including colony management, genotyping, brain slicing, slide mounting, just to name a few of the tasks with which your help was much appreciated. Thank you also to Valentine Greffion for your help with experimental planning and tissue collection, and for being great to work with. Thank you to Cameron Oram for your help with analyzing the behavioural data and for all your helpful advice and passionate discussions about neuroscience. Thank you to Kelvin Tian and George Sung for helping with lab work, and for being a fun bunch. Lastly, thank you to Cyril Bolduc for being a strong and focused presence in the lab, and for asking the tough questions!

I would also like to thank people outside of the Poulin Lab who helped over the course of my degree. Thank you to Kevin Lançon for all your help with fiber photometry. Thank you to the animal care staff at the MNI for always being available to help, especially Jessica, Fernando, and Eliana. Thank you GSAN for the fun stuff, and thank you Cédric Audy for all of your support.

Finally, thank you to my parents (Mommers and Babs!) for always believing in me.

"Our greatest weakness lies in giving up. The most certain way to succeed is always to try just one more time." – Thomas A. Edison

List of Figures

List of Abbreviations

AAV – Adeno-associated virus

AI – Artificial intelligence

ANOVA – Analysis of variance

ASD – Autism spectrum disorder

D1R – Dopamine 1 receptor

D2R – Dopamine 2 receptor

DA – Dopamine

DAergic - Dopaminergic

DAPI – 4',6-diamidino-2-phenylindole

DAT – Dopamine transporter

DStr – Dorsal striatum

FPSiT – frt loxP synaptophysin ires-Cre tdTomato (mouse line for synaptophysin-GFP expression)

GABA – Gamma-aminobutyric acid

L-DOPA – L-dihydroxyphenylalanine

MOR – Mu-opioid receptor

MSN – Medium spiny neuron

NAc – Nucleus accumbens

NIS – Nikon Imaging Software

OCT – Optimal cutting temperature compound

P0 – Postnatal day zero (day of birth)

PBS – Phosphate-buffered saline

PFA – Paraformaldehyde

RIM1 – Regulating synaptic membrane exocytosis 1

ROI – Region of interest

SHANK3 – Steroid receptor coactivator (SRC) homology domain 3 (SH3) and multiple ankyrin repeat domains 3

SNc – Substantia nigra pars compacta

Syn-GFP – Synaptophysin-linked green fluorescent protein

TH – Tyrosine hydroxylase

VGLUT2 – Vesicular glutamate transporter 2

VMAT2 – Vesicular monoamine transporter 2

VStr – Ventral striatum

VTA – Ventral tegmental area

Contribution of Authors

Sarah A. Martin (S.M.) performed all behaviour testing, performed all immunofluorescence experiments, took and analyzed all images, and ran all statistical analyses, unless otherwise stated. The following individuals contributed to this project: Dr. Jean-Francois Poulin, Lucia Guerra, Valentine Greffion, George Sung, Kelvin Tian, Cameron Oram.

Immunofluorescence and image analysis

JF.P. generated and validated Th-2A-Flpo mice and designed the project. S.M., L.G., and V.G. performed colony management, and S.M., L.G., V.G., K.T., and G.S. performed genotyping. L.G. set up breedings to generate Dat-Cre/Th-Flp/FPSiT mice. S.M., V.G., and L.G. developed the breeding scheme and set up breedings to generate Dat-Cre/Th-Flp/FPSiT/SHANK3b mutant mice. S.M. and V.G. euthanized mice and processed tissue. S.M., V.G., and L.G. performed brain slicing. S.M. performed immunofluorescence, and S.M., L.G., G.S., and K.T. performed slide mounting after immunofluorescence. S.M. and JF.P. developed the image analysis plan. S.M. took images, performed image analysis, performed statistical testing, and created all figures, except Figure 5A and 5B which were created by V.G.

SHANK3b mutant mice behavioural testing

S.M., L.G., and V.G. performed colony management, and S.M., L.G., V.G., K.T., and G.S. performed genotyping. S.M., L.G., and V.G. set up breedings to generate SHANK3b mutant mice for behavioural experiments. S.M. and L.G. performed animal habituation prior to testing, and S.M. performed behavioural testing. C.O. trained DeepLabCut AI and wrote MATLAB code to analyze behaviour videos. S.M. analyzed videos, performed statistical analysis, and created figures.

Introduction

Abnormal formation of dopamine (DA) circuits is hypothesized to underlie symptoms of autism spectrum disorder (ASD). However, DA synaptogenesis is poorly understood in normal development. Establishing how DA circuits are formed in development and how these circuits are affected in a mouse model of ASD will be critical to understand the symptoms of ASD. The aim of this study is to investigate the development of DAergic circuits in the striatum, specifically focusing on putative release sites of neurotransmitters from DAergic neurons, using an intersectional genetic mouse model that allows labeling of synaptic vesicles with green fluorescent protein (GFP). The development of glutamatergic circuits in the striatum has also been examined using immunofluorescence targeting of vesicular glutamate transporter 2 (VGLUT2). Three areas of the striatum have been analyzed: the dorsomedial striatum, the nucleus accumbens (NAc), and the patch-and-matrix structure of DAergic innervation in the striatum. The fluorescence intensity was analyzed in these areas in both normal mice and SHANK3b mutant mice, which is a mouse model of ASD, during early postnatal development. Additionally, SHANK3b mutant mice have been tested using a sociability assay to demonstrate the ASD-like behavioural phenotype seen in this mouse model.

Literature Review

The striatum: an overview

The striatum is a cluster of neurons acting as a major input structure of the basal ganglia, which plays a critical role in motor and reward systems (Cox & Witten, 2019). In rodents, the striatum can be subdivided into at least two areas based on function and connectivity: the dorsal striatum (DStr) and the ventral striatum (VStr). The DStr is usually known for its role in initiating and controlling bodily movement. The VStr, which contains the nucleus accumbens (NAc) and the olfactory tubercle, plays a role in motivation and reward. The NAc is often further divided into the NAc core and the NAc shell, each with different connectivity and functional roles (Mingote et al., 2019; Salgado & Kaplitt, 2015).

The main neurons of the striatum are the medium spiny neurons (MSNs), named "spiny" due to the presence of dendritic spines. These neurons release gamma-aminobutyric acid (GABA), and thus function as inhibitory (GABAergic) neurons. Most MSNs express either dopamine 1 receptor (D1R) or dopamine 2 receptor (D2R), with a smaller population recently found to express both D1 and D2 receptors (Bonnavion et al., 2023). The striatum also contains cholinergic and GABAergic interneurons which regulate MSN firing (Kandel et al., 2013). A subtype of GABAergic striatal interneurons expresses tyrosine hydroxylase (TH), which is an enzyme involved in the synthesis of several different neurotransmitters including dopamine (DA). However, these interneurons are not considered dopaminergic (DAergic) neurons because they do not express the other enzymes required to synthesize DA, nor the membrane transporters required to release it (Weihe et al., 2006; Xenias et al., 2015).

MSNs receive two types of input: excitatory input and modulatory input. Excitatory (glutamatergic) input to MSNs is received from the cortex and thalamus. MSNs in the NAc also

receive input from the amygdala, hypothalamus, and hippocampus (Modi & Sahin, 2019). Modulatory (DAergic) input to MSNs is received from DA neurons in the substantia nigra pars compact (SNc) and the ventral tegmental area (VTA) in the midbrain. MSNs send projections back into the midbrain, forming a feedback loop. DAergic neurons in the VTA preferentially project to the VStr (Chuhma et al., 2017). This is called the mesolimbic pathway, and is classically thought to play an important role in reward prediction error (Schultz, 2017). Current evidence also supports the involvement of the mesolimbic pathway in social behaviour (Gunaydin et al., 2014).

MSNs are not distributed homogenously within the striatum. Instead, MSNs are distributed in a patch-like pattern, where "patches" are referred to as striosomes and the surrounding area is referred to as the matrix (Märtin et al., 2019). MSNs within striosomes express mu-opioid receptor (MOR), and MSNs within the matrix express calbindin (Brimblecombe & Cragg, 2016). DAergic innervation of the striosomes and matrix is heterogenous: in the DStr, striosomes are innervated by neurons of the SNc (ventral), and the surrounding matrix is innervated by the VTA and the SNc (dorsal) (Jimenez-Castellanos & Graybiel, 1987). In the VStr, the distribution of MSNs also forms distinct patches, though their connectivity differs compared to the DStr. MSNs in striosomes of the VStr innervate DAergic neurons in the VTA, similar to how MSNs in striosomes of the DStr innervate DAergic neurons in the SNc (Watabe-Uchida et al., 2012). In summary, the striatum is a large input structure of the brain with massive excitatory and modulatory input, and cells within the striatum are segregated based on protein expression and connectivity.

DA synthesis and release

Modulation of striatal activity is facilitated by DA, and the synthesis of DA is well characterized. DA synthesis occurs in the cytosol of DAergic neurons. First, L-tyrosine is converted into L-dihydroxyphenylalanine (L-DOPA) via tyrosine hydroxylase (TH), and L-DOPA

is quickly converted to DA via DOPA decarboxylase (Ayano, 2016). DA is taken up into synaptic vesicles via vesicular monoamine transporter 2 (VMAT2), and synaptic vesicles localize to active zones along the axon, ready to be released (Kandel et al., 2013). Synaptophysin is a synaptic vesicle protein which is expressed widely in neurons, including DAergic neurons (Bai & Strong, 2014). Since synaptophysin localizes at release sites, the presence of synaptophysin can be used to quantify release sites in the brain (Valtorta et al., 2004). After release, dopamine transporters (DAT) on the pre-synaptic neuron remove excess DA from the extracellular space, so that it can be stored and released again (Best et al., 2009).

Expression of TH has classically been considered a marker for DAergic neurons; however, TH expression is not specific to DAergic neurons because TH is involved in the synthesis of two other catecholaminergic neurotransmitters, which are norepinephrine and epinephrine (Kandel et al., 2013). Additionally, a subset of GABAergic striatal and cortical interneurons express TH but do not synthesize DA, and some neurons (termed nonexocytotic catecholaminergic Th neurons) express TH and even synthesize DA but do not release DA (Weihe et al., 2006). The combination of both TH expression and DAT expression serves as a more specific marker for DAergic neurons which release DA (Kramer et al., 2021; Poulin et al., 2018), especially with the known limitations of current transgenic driver lines such as Th-Cre (Lammel et al., 2015).

DA axons form en-passant boutons, or varicosities, along the axon in a pattern sometimes called “beads on a string” due to its appearance (Liu et al., 2018). Traditionally, it is believed that DAergic neurons exert their influence in the brain using non-synaptic transmission, meaning that DA travels through extracellular space to activate distant targets instead of travelling across a synaptic cleft to a nearby post-synaptic cell (Vizi et al., 2010). However, recent evidence supports the idea that DA release only occurs at active zone-like areas on varicosities along the axon,

suggesting that DAergic neurons send signals via synaptic transmission rather than non-synaptic (Liu & Kaeser, 2019).

Development of the striatum

The development of the striatum has been thoroughly investigated (Knowles et al., 2021). MSN generation occurs mainly from E10.5 to birth (E19.5) in mice, though some MSNs are generated in early postnatal development (Wright et al., 2013). The birthdate of MSNs is a factor in determining their target location within the striatum. MSNs with an earlier birthdate are located in the caudal striatum (preferentially within striosomes) whereas MSNs with a later birth date are located in the rostral striatum (preferentially within the matrix) (Matsushima & Graybiel, 2020). Striatal interneurons are also organized heterogeneously between striosomes and matrix, including some interneurons which sit at the border between striosomes and matrix, and may serve as a bridge to modulate activity in both areas (Brimblecombe & Cragg, 2016). Synaptogenesis occurs postnatally, in which neurons create wide systems of circuits, and these circuits are later refined, or pruned, in which the number of synaptic connections is reduced (Kandel et al., 2013). Pruning occurs during a critical period in development, and problems during the pruning stage are implicated in several neurodevelopmental disorders including autism spectrum disorder (ASD) (Neniskyte & Gross, 2017; Tang et al., 2014).

MSN and dopaminergic circuit development

Previous research has investigated the development of DAergic circuits in the striatum using immunochemistry techniques to target DA and TH in rodent brains at different developmental timepoints (Antonopoulos et al., 2002; Fentress et al., 1981; Voorn et al., 1988). DAergic neurons send projections to the striatum by E17 in rats, and DAergic innervation of the

rostral striatum shows a ventrolateral to dorsomedial gradient, whereas DAergic innervation of the caudal striatum follows a ventromedial to dorsomedial and lateral gradient (Voorn et al., 1988). By E19 in rats, patches of DAergic innervation start to become visible in the dorsolateral striatum, and these patches start to appear medially into post-natal development (Voorn et al., 1988). This "patch and matrix" pattern of DAergic innervation persists through the first two to three weeks of life, and by P21, patches of DA innervation are no longer detectable with DA staining (Antonopoulos et al., 2002). Varicosities first appear on DAergic axons postnatally and then quickly increase in number until reaching near adult levels by about three weeks of age (Voorn et al., 1988). DA circuit development is not limited to perinatal timepoints, as research has shown that DA circuits continue to develop and mature throughout adolescence and into adulthood (Reynolds & Flores, 2021).

DA release in the striatum does not begin until about P6 to P10, after which it increases to a steady rate until P18, and this increase of DA release in the striatum coincides with the formation of MSN spines which is reported to occur between P11 and P20 in rats (Kim et al., 2002; Lieberman et al., 2018; Tepper & Trent, 1993). As the spines of MSNs form, the number of synapses from DAergic axons to MSN spines increases, which suggests that DA circuit maturation in the striatum is an active process related to the development of MSNs (Antonopoulos et al., 2002). Indeed, research has shown that DA is required for the normal development of MSNs from an immature, hyperexcitable state to a mature, lower excitability state (Lieberman et al., 2018). This demonstrates the importance DA in striatal development, particularly regarding the development of MSNs.

In sum, the pattern of DAergic circuit development in the striatum has been elucidated using TH and DA immunolabeling, but the distribution of release sites on striatal DAergic

projections during development has not been characterized. Additionally, research has shown that DA is important for the proper development of MSNs, which suggests that improper MSN development may be related to aberrant DA release within the first few weeks of life.

Glutamate co-transmission

DAergic neurons in the midbrain are not homogenous. Rather, several subtypes of DA neurons exist, and they can be grouped into categories according to their particular transcriptomic signature (Poulin et al., 2020). Some DA neurons express the gene *Slc17a6* which encodes for vesicular glutamate transporter 2 (VGLUT2), which is responsible for the uptake of L-glutamate into synaptic vesicles. These VGLUT2+ DA neurons therefore release both DA and glutamate. Glutamatergic co-release from DAergic neurons was first discovered in the late 1990s (Sulzer et al., 1998) and has since been studied in more depth. VGLUT2+ DA neurons are mainly located in the VTA, and account for 10-30% of the DA neurons in this area (Eskenazi et al., 2021). VGLUT2+ DA neurons of the VTA project mainly to the medial shell of the NAc (Poulin et al., 2018). Interestingly, nearly all midbrain DAergic neurons express VGLUT2 during pre-natal development (Kouwenhoven et al., 2020). This suggests a possible role of glutamate co-transmission in the proper development of DAergic circuits, although it is not clear at which point during development glutamate is released in the striatum by DAergic neurons. Conditional knock-out (KO) of *Vglut2* in midbrain DAergic neurons during embryonic development reduces reinnervation in the striatum after a lesion elicited by a neurotoxin (Kouwenhoven et al., 2020) which supports the idea that VGLUT2 is important for neural growth and plasticity. The role of glutamate co-transmission in DAergic neurons is an ongoing area of research.

It is still unclear whether DA and glutamate are released from the same or separate sites on the DA neuron axon, although *in vivo* and *in vitro* evidence suggest that DA and glutamate release

sites are mostly segregated (Fortin et al., 2019; Zhang et al., 2015). Interestingly, Fortin et al. (2019) also showed *in vitro* that the segregation of DA and glutamate release sites is regulated by contact with MSNs in the striatum, and the expression of VGLUT2 is also regulated by MSNs in the dorsal striatum. This finding has implications regarding the normal development of DAergic circuits, and the importance of proper contact with target cells in how these circuits develop.

Autism Spectrum Disorder

ASD is a neurodevelopmental disorder characterized by two core symptoms, which are repetitive motor behaviour and deficits in social interaction and communication (American Psychiatric Association, 2013). The behavioural features of ASD emerge through development (Ozonoff et al., 2010) which strongly indicates that the root of ASD is a difference in how the brain develops in ASD versus neurotypical children. The symptoms of ASD persist throughout the lives of those affected. It is commonly reported that the ratio of boys to girls with ASD in the United States is 4.3 to 1 (Maenner et al., 2020). However, this ratio has been debated: some sources indicate the true sex difference is lower at 2:1 or 3:1 with males still showing a higher prevalence compared to females (Halladay et al., 2015).

Alterations to neural organization have been reported in ASD. Port-mortem analysis of the striatum in young patients diagnosed with ASD has revealed that the distinction between patch and matrix components is less segregated compared to control brains (Kuo & Liu, 2020). Differences in brain volume between ASD and neurotypical children have also been investigated (Sparks et al., 2002). Several studies have found an increase in the volume of the striatum in patients with ASD, particularly the caudate nucleus (a structure of the dorsal striatum) (Hollander et al., 2005; Langen et al., 2009). Some recent research has found that the volume of the ventral striatum is decreased in children with ASD, and that this difference is correlated with the severity

of their deficits in social communication (Baribeau et al., 2019). The results of these neuroimaging studies provide some interesting insight into the brain regions involved in ASD, however, these studies are only correlational. More specific insight on differences in the brain between ASD and neurotypical individuals may be gleaned by investigating neural circuits.

Dopamine and social behaviour in ASD

The DA hypothesis of ASD posits that the dysregulation of DA circuits may play a role in the behavioural symptoms of ASD (Pavăl, 2017). This hypothesis rests on the established role of the striatum (which receives strong DAergic innervation from the midbrain) in motor control and social behaviour, the two main behavioural domains affected by ASD. Dysregulation of the mesolimbic pathway, for example, could alter the value assigned to social stimuli, which is typically high enough to encourage an individual to seek and engage in social interaction. Individuals with an altered valence to social stimuli might develop deficits in social communication due to a disinterest in engaging in social behaviour during childhood, when these skills are typically learned.

In patients with ASD, neural activity during social tasks is altered. Activity in the striatum which would typically by elicited by social stimuli is reduced in young patients with ASD, and this was found in multiple studies using functional magnetic resonance imaging (fMRI) (Kohls et al., 2013; Scott-Van Zeeland et al., 2010; Zürcher et al., 2021). In mice, activity of DAergic neurons in the mesolimbic circuit has been shown to play a role in social behaviour (Dai et al., 2022; Gunaydin et al., 2014) but whether the activity of the mesolimbic circuit is altered in ASD during social behaviour remains unknown.

SHANK3 and ASD

ASD is highly heritable, and nearly 1000 genes have been associated with the disorder (Arpi & Simpson, 2022). Many of the genes linked with ASD contribute to brain development and synaptic function (Quesnel-Vallières et al., 2018). One such gene is *Shank3*. Disruption of the *Shank3* gene in humans results in Phelan-McDermid syndrome, and one of the symptoms of this syndrome is ASD (Phelan & McDermid, 2012). *Shank3* encodes for the scaffolding protein SHANK3 located at the post-synaptic side of glutamatergic synapses (Boeckers, 2006). The SHANK3 protein contains a PDZ domain, which is implicated in the assembly of the post-synaptic density (PSD) scaffold complex, as well as multiple ankyrin repeats, which mediate protein-protein interactions (Peça et al., 2011). Expression of *Shank3* at P14 in mice is highest in the striatum compared to other brain structures (Zhao et al., 2017) and continues to be highly expressed in the striatum in adulthood (Peça et al., 2011). *Shank3* is also expressed on DAergic neurons in the midbrain (Bariselli et al., 2016)

Peça et al. (2011) generated a *Shank3* mutant strain of mice (SHANK3b mutant mice) by replacing the section of the *Shank3* gene that encodes the PDZ domain with a neo cassette, resulting in a complete knockout of two isoforms of the SHANK3 protein family (alpha and beta) as well as a reduction of the gamma isoform. This mutation produces ASD-like symptoms, such as repetitive grooming and social behaviour deficits, as well as decreased spine density on MSNs in the DStr (Peça et al., 2011). This mouse model has since been used in multiple studies to investigate cellular and behavioural disruptions related to *Shank3* mutation (Balaan et al., 2019; Bukatova et al., 2021; Peixoto et al., 2019) ASD-like symptoms are also observed in non-human primates with mutation of *Shank3* (Zhou et al., 2019). Thus, *Shank3* mutant animals can be used to investigate the neural basis of ASD-related symptoms.

SHANK3 and the mesolimbic pathway

Since SHANK3 is a post-synaptic protein at glutamatergic synapses, Vglut2+ DA neurons of the VTA are of special interest in the study of *Shank3* mutation for two reasons. First, Vglut2+ DA neurons form the pre-synaptic side of glutamatergic synapses in the VStr (Mingote et al., 2019). Second, Vglut2+ DA neurons form the post-synaptic side of glutamatergic synapses in the VTA (Bariselli et al., 2016).

In the VStr, Vglut2+ DA neurons form glutamatergic synapses onto MSNs and cholinergic interneurons. Research suggests that glutamatergic activation from Vglut2+ DA neurons is stronger on cholinergic interneurons than MSNs (Mingote et al., 2019). The proposed function of cholinergic interneurons in this local circuit is to modulate the firing of DAergic neurons onto MSNs (Mingote et al., 2019). Mutation of *Shank3* may affect synapses between Vglut2+ DA neurons and cholinergic interneurons, thereby affecting the release of DA onto MSNs. This would ultimately alter how DAergic circuits modulate the firing of MSNs in the VStr and could play a role in behavioural deficits associated with this region of the striatum, such as social behaviour deficits.

In the VTA, downregulation of SHANK3 during early postnatal development negatively affects excitatory synapse maturation on DA neurons, resulting in decreased burst activity and a social behaviour deficit (Bariselli et al., 2016). In the same study, the authors found that optogenetic activation of DA neurons in the VTA of SHANK3-downregulated mice was sufficient in rescuing the social behaviour deficit (Bariselli et al., 2016). These findings highlight the role of SHANK3 in proper development and functioning of the DAergic mesolimbic circuit.

Additionally, striatal neurons regulate the segregation of DAergic and glutamatergic release sites on Vglut2+ DA neurons through synaptic contact (Fortin et al., 2019). *Shank3*

mutation alters striatal synapses, thus improper synaptic contact may alter how DAergic and glutamatergic release sites are segregated. This could in turn affect the proper development and function of Vglut2+ DAergic neurons. The relationship between *Shank3* mutation and DAergic circuit development, particularly regarding DA neuron subtypes, is yet to be fully elucidated.

Objectives of the current study

This study aims to investigate the development of DAergic circuits, and how this development may be altered in SHANK3b mutant mice, a mouse model of ASD. To achieve this goal, a reporter mouse has been used to visualize putative release sites of DA on striatal DAergic projections at early postnatal timepoints (P0 and P14). The distribution of VGLUT2 in the striatum during postnatal development is also investigated, in both normal mice and SHANK3b mutant mice.

Methods

Mouse strains, breeding schemes, and colony management

The use of animals in this project adheres to the guidelines published by the Canadian Council of Animal Care, and all operating procedures were approved by the Montreal Neurological Institute Animal Care Committee. Mice were housed at constant temperature and humidity on a 12-hour light-dark cycle with *ad libitum* access to food and water. Behavioural testing was performed during the light portion of the cycle between 8:00am and 6:00pm. C57BL/6 mice were obtained from Charles River Laboratories and bred in-house with Dat-ires-Cre (Bäckman et al., 2006) and Th-2A-Flpo mice (Poulin et al., 2018), then crossed to generate Dat-Cre/Th-Flp mice. RC::FPSiT mice were originally obtained from The Jackson Laboratory (JAX stock #030206; Niederkofler et al., 2016) and bred in-house with Dat-ires-Cre/Th-2A-Flpo mice to generate Dat-Cre/Th-Flp/FPSiT mice.

SHANK3b mutant mice were obtained from The Jackson Laboratory (JAX stock #017688; Peça et al., 2011) and used in two separate breeding schemes to generate experimental mice for this project. First, SHANK3b mutant mice were bred in-house with Dat-ires-Cre mice to generate Dat-Cre/SHANK3b mutant mice. Second, Th-Flp/FPSiT animals generated from the previously mentioned Dat-Cre/Th-Flp/FPSiT breeding were bred with SHANK3b mutant mice to generate Th-Flp/FPSiT/SHANK3b mutant mice. Lastly, Dat-Cre/SHANK3b mutant mice were crossed with Th-Flp/FPSiT/SHANK3b mutant mice to generate Dat-Cre/Th-Flp/FPSiT/SHANK3b mutant mice.

Behavioural testing and analysis

To test sociability, the three-chamber sociability test was used (Rein et al., 2020) (Figure 1). The control mice used were Dat-Cre/SHANK3b WT (n = 5; 3 males, 2 females) and

experimental mice were Dat-Cre/SHANK3b mutant (n = 7; 4 males, 3 females), hereafter referred to as WT and SHANK3b mutant respectively. These mice underwent invasive surgery 6 weeks before testing (stereotaxic injection of an adeno-associated virus and fiber optic implantation) and were connected to a fiber optic cable for the duration of the test. The purpose of this was to measure DAergic activity in the NAc during social behaviour via fiber photometry. However, the fiber photometry data was insufficient for inclusion in the current study. As such, only the results of the behaviour analysis will be reported.

Designated stranger mice (unfamiliar to the test mouse) were sex-matched and age-matched to test mice within 2 weeks of age at most. Each day for the 3 days preceding the test, stranger mice were placed in chambers for 20 minutes to allow habituation to the test environment. Similarly, test mice were habituated to the testing box without chambers each day for 30 minutes (the fiber optic implant was attached to an overhanging patch cable for the duration of habituation). On the day of the test, all mice (test mice and stranger mice) were acclimated to the behaviour testing room for at least 1 hour in their home cages. At the start of the test, the test mouse (after being attached to the overhanging patch cable) was placed in the test box with chambers placed on opposite sides of the box, and the mouse was allowed to explore freely for 10 minutes (Phase 1) while the investigator waited in a separate room. The session was performed in the dark and was video recorded using an infrared camera. At the end of Phase 1, the lights were turned on and the mouse was moved to a nearby cage with a small amount of home bedding while the testing box and chambers were cleaned with 75% ethanol to remove animal scents. The test box was dried completely with paper towels, then two clean sheets of paper towel were used to create two paper balls, placed in the centre of each of the chambers within the test box. The mouse was placed in the test box and allowed to explore freely for another 10 minutes, in the dark and video recorded

in infrared while the investigator was absent (Phase 2). The mouse was then moved back to the same nearby cage as after Phase 1 and the test box and chambers cleaned again with 75% ethanol, and paper balls discarded. The designated stranger mouse was placed in one of the empty chambers, while an unfamiliar object (either a jumbo blue LEGO brick or a metal clamp of similar size and shape) was placed in the other empty chamber, and the test mouse was reintroduced to the test box to explore freely for another 10 minutes in the dark with infrared video recording while the investigator was absent (Phase 3). At the conclusion of the test, all mice were returned to their respective home cages and the test box, chambers, and items were cleaned with 75% ethanol.

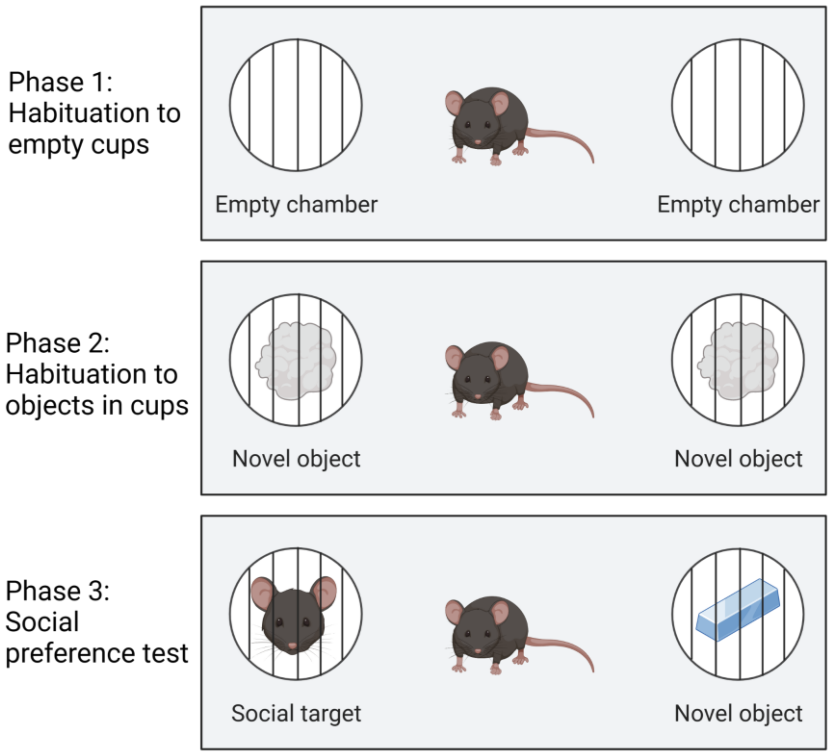

Figure 1. Schematic demonstrating the three phases of the 3-chamber sociability test designed to assess social preference, as described in Rein et al. (2020). Created with BioRender.com.

DeepLabCut artificial intelligence (AI) (Mathis et al., 2018) was trained to recognize the nose position of the test mouse, and then used to measure the duration of time that the test mouse spends interacting with each chamber (i.e. when the nose of the test mouse is within the perimeter of the chamber) in each phase of the test. The proportion of time spent interacting with each chamber was calculated by dividing the duration of interaction time by the total duration of the mouse exploring the test box, then subjected to two-way ANOVA followed by post-hoc Bonferroni tests using GraphPad Prism 9.4.1. Traces of mouse travel in the test box were generated using DeepLabCut and custom script in MATLAB. Sexes were combined for analysis in the current study to achieve an acceptable number of mice for each group (WT and SHANK3b mutant).

Tissue processing and immunofluorescence

Whole brains of Dat-Cre/Th-Flp/FPSiT mice have been collected at specific timepoints (P0, P14, P21). Timepoints were selected based on developmental milestones that occur in the striatum and DAergic system during early post-natal development (Figure 2). Brains of Dat-Cre/Th-Flp/FPSiT/SHANK3b mice have been collected at P0 and P14 to be compared to Dat-Cre/Th-Flp/FPSiT mice (n = 4 for each of P0 and P14; 3 males and 1 female in each group, except for Dat-Cre/Th-Flp/FPSiT at P0 in which all 4 mice are male). Sex of mice at P0 were determined using the method described in Wolterink-Donselaar et al. (2009).

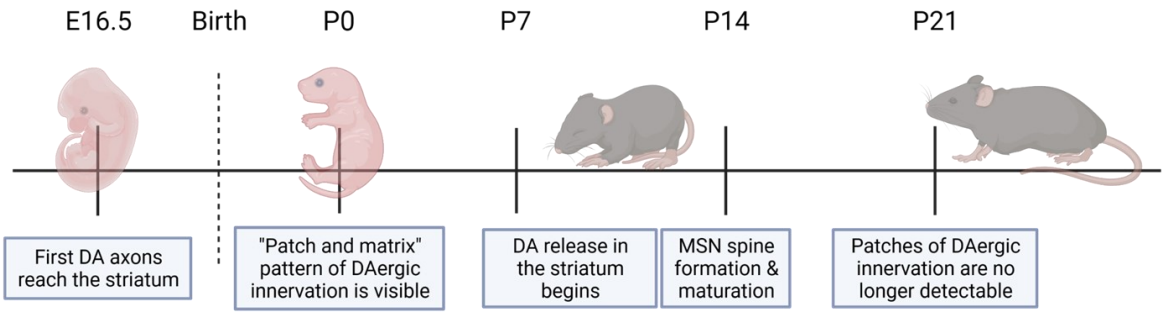

Figure 2. Timeline summarizing major milestones of DA circuit development in the striatum during late prenatal and early postnatal growth. Created with BioRender.com.

Tissue processing and immunofluorescence procedure for P0 mice: Mice were anesthetized using ice to induce hypothermia, then decapitated to allow the brain to be collected. The brain was immediately placed in ice-cold 4% paraformaldehyde (PFA) and refrigerated at 4 degrees Celsius overnight, and then dehydrated in a 30% sucrose solution at 4 degrees Celsius until the brain has sunk in the solution (48-72 hours). The brain was then removed from 30% sucrose and frozen in optimal cutting temperature compound (OCT) at -80 degrees Celsius, then sliced on a cryostat in 25um sections. Slices were immediately mounted on slides and stored in a sealed slide box at -80 degrees Celsius until use.

All P0 mice in this study were stained simultaneously. To perform immunofluorescence, slides were thawed at room temperature for at least 30 minutes and then placed in an upright slide holder and washed with 1X PBS for 10 minutes, followed by 4% PFA for 20 minutes, and then 2 more washes of 5 minutes each in 1X PBS. Slides were then placed flat in a slide box and sections are incubated in blocking solution (1X PBS + 0.3% Triton-X + 5% normal donkey serum) for 1 hour at room temperature. Blocking solution was then removed from slides and sections were then incubated in primary antibody solution containing anti-GFP (chicken, 1:2000 dilution, Abcam #ab13970), anti-TH (sheep, 1:500 dilution, Pel-Freez #P60101), and anti-VGLUT2 (rabbit, 1:1000

dilution, Synaptic Systems #135402), overnight at 4 degrees Celsius. After overnight incubation, slides were moved to upright slide holder and washed 4 times for 5 minutes each time with 1X PBS + 0.05% Tween-20 before being placed flat and incubated with secondary antibody solution containing donkey anti-chicken Alexa 488 (1:250 dilution, Jackson Immuno #703-545-155), anti-sheep Alexa 568 (1:250 dilution, Invitrogen #A21099), and anti-rabbit Alexa 647 (1:250 dilution, Invitrogen #A31573) for 2 hours at room temperature. After secondary antibody incubation, slides were returned to upright slide holder and washed 4 times for 5 minutes each time with 1X PBS + 0.05% Tween-20 followed by a 5 minute wash with 1X PBS. Slides were then coverslipped immediately with mounting media containing DAPI (Abcam #ab104139-100ML), sealed with clear nail polish, and laid flat to dry overnight before moving to a slide box and stored at 4 degrees Celsius until imaged.

Tissue processing and immunofluorescence procedure for P14 and P21 mice: Brains were collected following whole animal intracardiac perfusion with 25mL 1X PBS followed by 75mL 4% PFA (both chilled on ice), after which the brain was fixed overnight in 4% PFA at 4 degrees Celsius and then dehydrated in a 30% sucrose solution at 4 degrees Celsius until the brain has sunk in the solution (48-72 hours). The brain was then frozen at -80 degrees Celsius and sliced on a microtome at 25um. After slicing, brain slices were stored free-floating in cryoprotectant solution at -20 degrees Celsius until use.

All P14 mice in this study were stained simultaneously. Additionally, all the following immunofluorescence steps (before slide mounting) were performed on a stir plate at room temperature unless otherwise stated. Brain sections were removed from cryoprotectant solution and washed 3 times for 10 minutes each time in 1X phosphate-buffered saline (PBS). Then, sections were incubated in blocking solution (PBS 1X + 0.3% Triton-x + 5% normal donkey

serum) for 30 minutes. After incubating in blocking solution, sections were incubated in primary antibody containing anti-GFP (chicken, 1:2000 dilution, Abcam #ab13970), anti-TH (sheep, 1:500 dilution, Pel-Freez #P60101), and anti-VGLUT2 (rabbit, 1:1000 dilution, Synaptic Systems #135402) overnight on a stir plate at 4 degrees Celsius. After overnight incubation, sections were washed in 1X PBS + 0.05% Tween-20 4 times for 5 minutes each time, then incubated for 2 hours in secondary antibody solution containing anti-chicken Alexa 488 (1:250 dilution, Jackson Immuno #703-545-155), anti-sheep Alexa 568 (1:250 dilution, Invitrogen #A21099), and anti-rabbit Alexa 647 (1:250 dilution, Invitrogen #A31573), followed by 3 washes of 5 minutes each in 1X PBS + 0.05% Tween-20 and one final wash of 5 minutes in 1X PBS. Sections were then mounted on slides in 1X PBS immediately or within 48 hours (sections that were not mounted immediately were stored in 1X PBS at 4 degrees Celsius until mounted). Slides were then coverslipped using either gelvatol or mounting media with DAPI (Abcam #ab104139-100ML), then sealed with clear nail polish before being placed flat and left to dry at room temperature overnight, then stored at 4 degrees Celsius in a slide box until microscope images were taken.

Image acquisition and analysis

Fluorescence intensity has been analyzed in pre-determined areas of the striatum of control and SHANK3b mutant mice (Figure 3A). Four regions of the striatum along the rostral-caudal gradient have been selected for analysis, beginning rostrally before the corpus callosum crosses into both hemispheres, and ending caudally at the tail of the striatum. These four levels of the striatum have been denoted as L1, L2, L3, and L4 (Figure 3B). L4 was not analyzed in P0 due to inconsistent tissue quality.

To analyze fluorescence intensity, low-magnification confocal images (4x magnification) have been taken using a Nikon Ti2 confocal microscope. Using NIS Elements analysis software,

square-shaped regions of interest (ROIs) were manually placed on these images and the mean fluorescence intensity within each ROI was measured. For dorsomedial striatum, matrix, and NAc lateral shell, ventral shell and core, a square ROI of equal size and placement within the structure was used across all animals. For patches and the dorsomedial shell of the NAc, a custom ROI was manually traced around the structure.

The values for mean fluorescence intensity within each ROI were exported to GraphPad Prism 9.4.1 software for statistical analysis. Fluorescence intensity of the corpus callosum in each image was used to correct all measurements against background fluorescence. For analysis of the dorsomedial striatum at P0 and P14, one sample t-tests were used to determine whether the mean intensity of each channel is statistically different from zero. For analysis of the NAc at P14, two-way ANOVA with post-hoc Tukey tests were used for each channel separately (Syn-GFP, TH, and VGLUT2). For analysis of patch and matrix at P0 and P14 across rostral-caudal levels L1 to L4, the anticipated statistical test was a repeated measures one-way ANOVA with post-hoc Tukey's tests. However, some values were missing due to poor tissue quality or absence of an appropriate slice, and datasets with missing values cannot be analyzed using a repeated measures ANOVA. Instead, the data was analyzed by fitting a mixed model to the data in GraphPad Prism. The results of a mixed model analysis can be interpreted similarly to a repeated measures ANOVA (GraphPad Software, Inc.). Post-hoc Bonferroni's tests were run to compare the difference in fluorescence intensity between patches and matrix for each level of the striatum. Due to low availability of mice, sexes were combined for analysis to achieve an acceptable number of subjects per group (Dat-Cre/Th-Flp/FPSiT and Dat-Cre/Th-Flp/FPSiT/SHANK3b mutant).

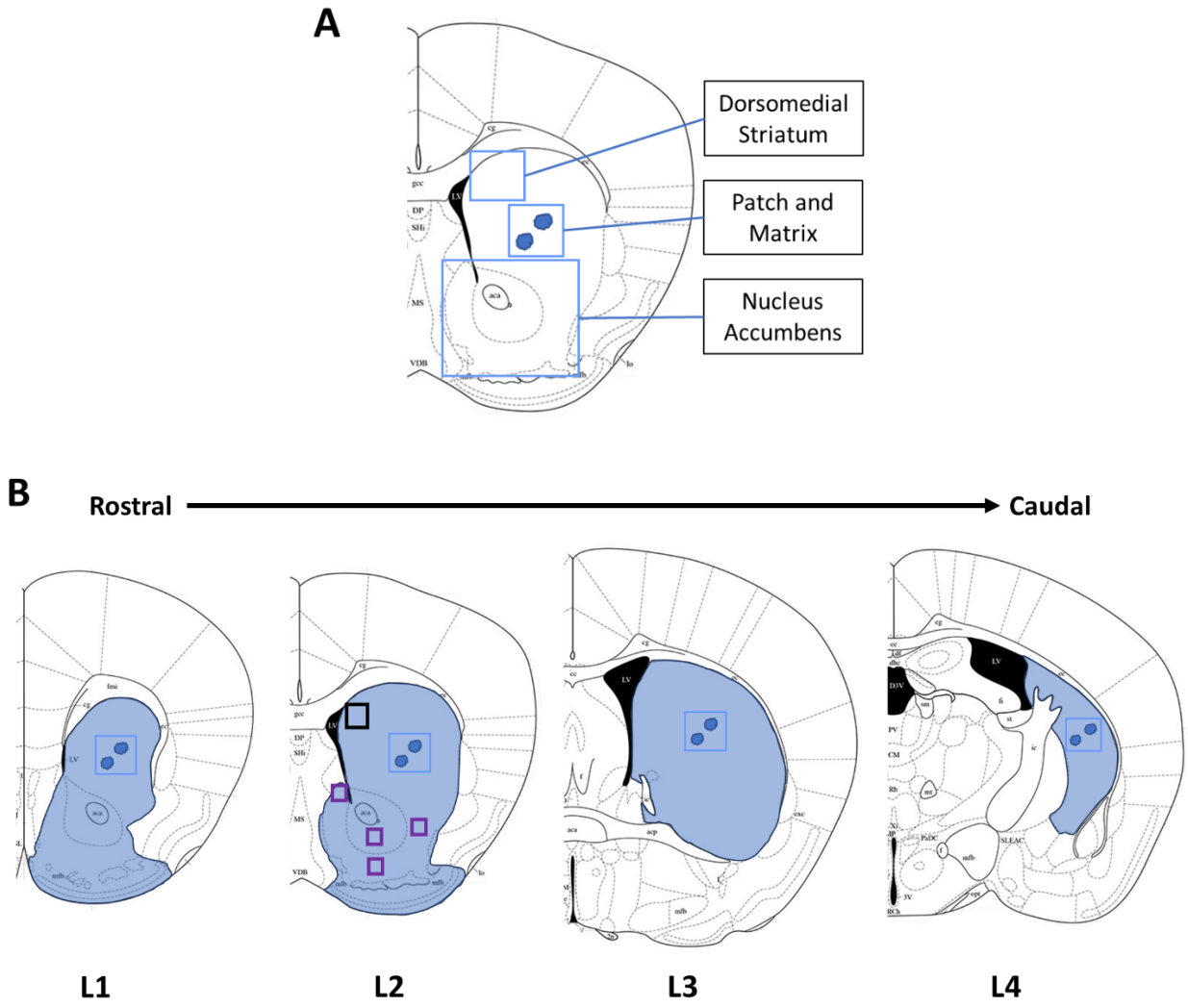

Figure 3. Schematic demonstrating the fluorescence intensity analysis plan. (A) Pre-determined areas of the striatum selected for fluorescence intensity analysis. (B) Striatum at different rostral-caudal levels (denoted L1 through L4), highlighted in blue. Placement of ROI for dorsomedial striatum indicated by black square, and placement of ROIs for different areas of the nucleus accumbens (NAc) indicated by purple squares in L2. Patches and matrix were analyzed across L1-L3 for P0 and L1-L4 for P14, represented by blue squares. Adapted from Paxinos & Franklin (2001).

Results

SHANK3b mutant mice demonstrate a deficit in social behaviour in the modified 3-chamber sociability test

It is important to validate the behavioural phenotype of SHANK3b mutant mice in the lab to ensure that the mice we are using for this study show traits of ASD as expected. To do this, a modified version of the 3-chamber sociability test has been used (Rein *et al.*, 2020). In the 3-chamber sociability test, the test mouse is simultaneously presented with two stimuli in chambers on opposite sides of the testing box: a social stimulus (stranger mouse) and a non-social stimulus (a novel object). The mouse is allowed to freely explore the testing box and two chambers. A typical wildtype (WT) mouse is expected to prefer to spend time with the social stimulus versus the non-social stimulus, whereas a mouse exhibiting a social behaviour deficit is not expected to prefer the social stimulus over the non-social stimulus. The modified version of this test includes two phases (Phase 1 and Phase 2) before the introduction of the social stimulus, to habituate the animal to the presence of chambers in the test box (Phase 1) and to the presence of identical novel objects within the chambers (Phase 2).

The results from Phase 1 of the 3-chamber sociability test show that there were no significant interaction effects between chamber (left versus right) and mouse genotype (WT versus SHANK3b mutant) on the proportion of time spent interacting with each chamber (Figure 4A, WT: n = 4; SHANK3b mutant: n = 5, $F_{1,14} = 0.8$, $P > 0.3$, two-way ANOVA, non-significant interaction effect). Main effects analysis shows no significant effect of left versus right chamber on proportion of time spent interacting with a chamber (Figure 4A, WT: n = 4; SHANK3b mutant: n = 5, $F_{1,14} = 0.7$, $P > 0.4$, two-way ANOVA, non-significant effect of chamber). Overall, these results show that WT and SHANK3b mutant mice do not spend more time interacting with either the right or left chamber when both are empty.

The results from Phase 2 show no significant interaction effects between chamber and mouse genotype (Figure 4B, WT: n = 5; SHANK3b mutant: n = 7, $F_{1,20} = 0.7$, $P > 0.4$, two-way ANOVA, non-significant interaction effect). Main effects analysis of left versus right chamber shows no significant effect of left versus right chamber on the proportion of time spent interacting with a chamber (Figure 4B, WT: n = 5; SHANK3b mutant: n = 7, $F_{1,20} = 1.0$, $P > 0.3$, two-way ANOVA, non-significant effect of chamber). These results show that WT and SHANK3b mutant mice do not prefer interacting with either the right or left chamber when both contain identical novel objects.

The results from Phase 3 show a significant interaction effect between chamber and mouse genotype (Figure 4C, WT: n = 5; SHANK3b mutant: n = 7, $F_{1,20} = 7.0$, $P < 0.02$, two-way ANOVA, significant interaction effect). Post-hoc Bonferroni's tests show that WT mice spend a higher proportion of time interacting with the social stimulus (Stranger) compared to the novel object (Figure 4C, adjusted p-value < 0.001) whereas SHANK3b mutant mice do not spend a higher proportion of time interacting with the social stimulus compared to the object (Figure 4C, adjusted p-value > 0.9). This demonstrates that SHANK3b mutant mice are less interested in a social stimulus versus a non-social stimulus compared to wildtype mice, reflective of what was previously reported in this and other mouse models of ASD (Balaan et al., 2019; Peça et al., 2011; Rein et al., 2020).

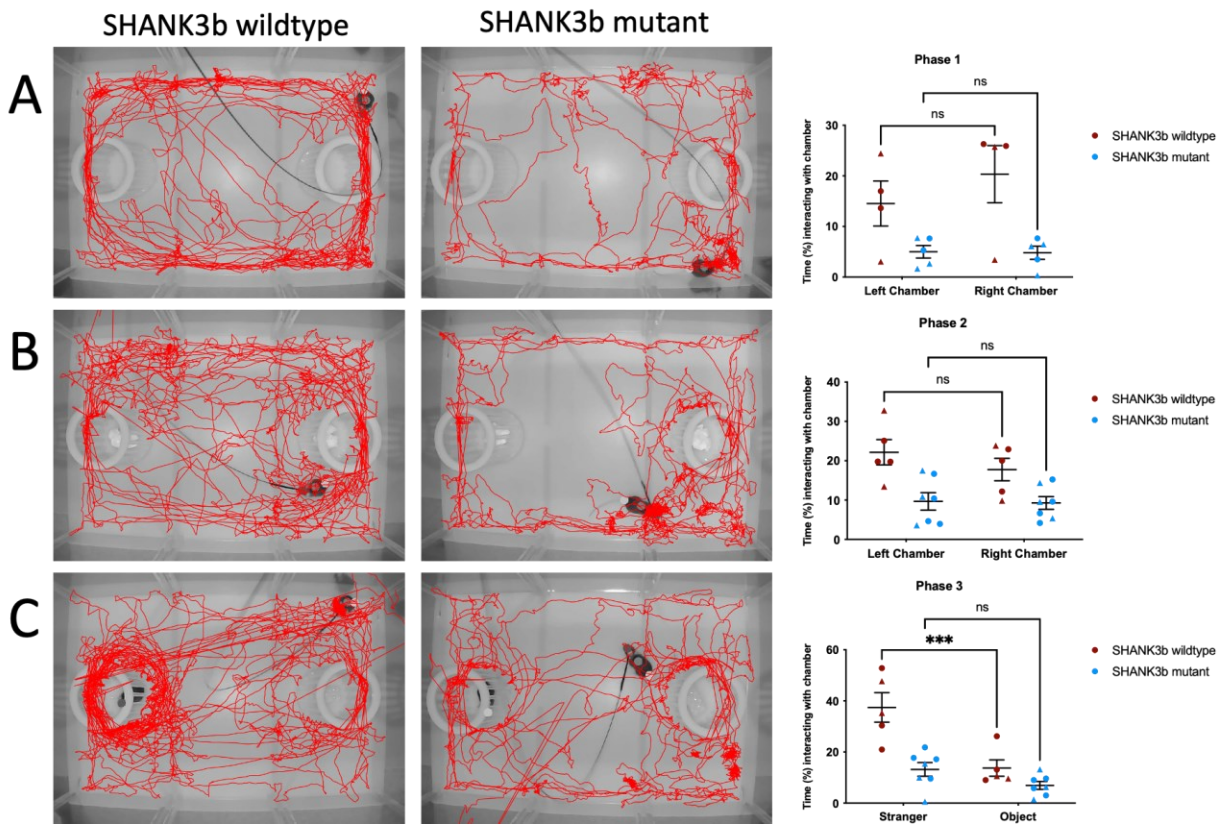

Figure 4. Results from the 3-chamber sociability test, showing that SHANK3b wildtype mice display a social preference whereas SHANK3b mutant mice do not. Phase 1-3 of the test are represented by rows A-C respectively. Representative motion trace of a test mouse during each phase is shown for both a SHANK3b wildtype and a SHANK3b mutant mouse. Data represent proportion of time (%) spent interacting with each chamber over the duration of each test phase, presented as mean +/- SEM. *** $p < 0.001$, ns, no significant difference. Circles denote males, triangles denote females.

Investigating the development of DA circuits in an intersectional genetic mouse model

The development of DA circuits can be visualized using intersectional genetics with a reporter mouse strain (RC::FPSiT). To visualize DAergic projections, RC::FPSiT mice have been crossed with Dat-Cre and Th-Flpo mice, such that the presence of both Cre and Flp recombinases in RC::FPSiT mice results in the expression of the fusion protein eGFP linked to synaptophysin (Syn-GFP) (Figure 5A). Synaptophysin is located on synaptic vesicles which typically localize to the active zones of the pre-synaptic terminals and varicosities where neurotransmitters are released

(Figure 5B). Thus, this intersectional genetic method allows us to specifically target midbrain DA neurons that express both *Dat* and *Th*, and visualize neurotransmitter release sites using immunofluorescence with confocal microscopy (Figure 5C).

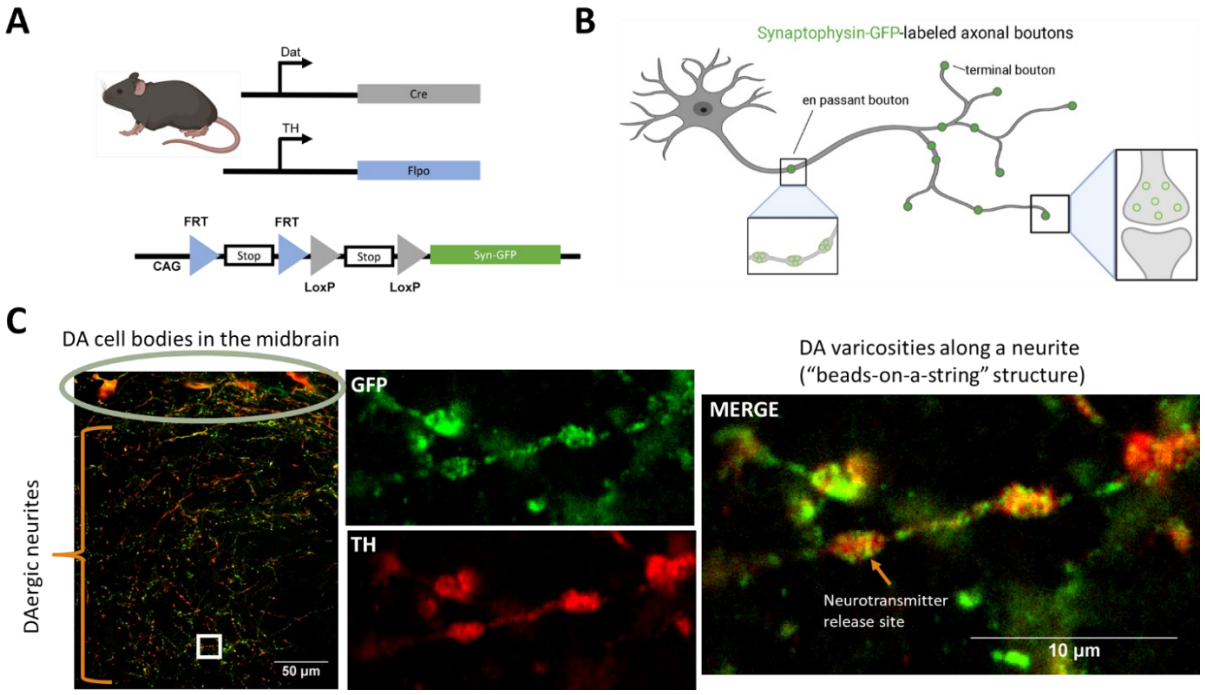

Figure 5. Reporter mouse strain used to target neurotransmitter release sites on midbrain DAergic neurons. (A) Schematic demonstrating the transgenic mouse line Dat-Cre/Th-Flp/FPSiT. Expression of both Cre and Flp recombinases in RC::FPSIT mice results in the expression of Syn-GFP. (B) Syn-GFP allows the visualization of presynaptic neurotransmitter vesicles at axon terminals and en passant boutons (varicosities) along the axon of DAergic neurons. (C) Confocal image of DAergic neurites in the midbrain of a Dat-Cre/Th-Flp/FPSiT mouse (P21), stained for GFP (green) and Th (red) using immunofluorescence. Pop-out image shows clusters of Syn-GFP are clearly visible within varicosities, marked by orange arrow. (A) and (B) created by Valentine Greffion with BioRender.com.

Development of DAergic and glutamatergic innervation in the striatum at P0, P14, and P21

To investigate the development of DAergic and glutamatergic innervation of the striatum through postnatal development, triple immunofluorescence was performed on sections of Dat-Cre/Th-Flp/FPSiT mouse striatum at P0, P14, and P21, staining for Syn-GFP (to enhance endogenous fluorescence), TH, and VGLUT2.

At P0, Syn-GFP is densely present in patches in the striatum and less dense in the surrounding matrix, and at P14 these patches continue to be visible though they are less visually distinguishable from the surrounding matrix (Figure 6, green arrows). Both TH and VGLUT2 are present in patches at P0, but by P14, VGLUT2 is no longer densely present in patches and instead appears to be denser in the surrounding matrix (Figure 6, blue arrows). Notably, the expression pattern of Syn-GFP and TH is not identical, demonstrating the power of this intersectional genetic technique to better visualize release sites on DAergic projections compared to visualizing all Th-positive neural projections. For example, there is dense Th expression ventromedially to the striatum, and this area does not appear to have significant Syn-GFP expression (Figure 6, red arrows). At P0, the ventral striatum is underdeveloped – the landmark structures of the NAc (core and shell) are not clearly defined by DAergic or glutamatergic innervation at this timepoint. At P14, the ventral striatum is well defined by DAergic and glutamatergic innervation – the core and shell of the NAc are visible and resembles the shape and innervation pattern of the NAc in adulthood, and VGLUT2 is densely present in the medial shell of the NAc (Figure 6, white dotted outline). Finally, the dorsomedial aspect of the striatum at P0 almost completely lacks DAergic and glutamatergic innervation, whereas at P14, DAergic and glutamatergic innervation is present in the dorsomedial striatum (Figure 6, white asterisk).

Overall, this series of images demonstrates the pattern of development of the striatum postnatally from birth to 3 weeks of age. In the following sections, fluorescence intensity of three areas of the striatum will be analyzed: the dorsomedial striatum, the NAc, and the patch and matrix pattern.

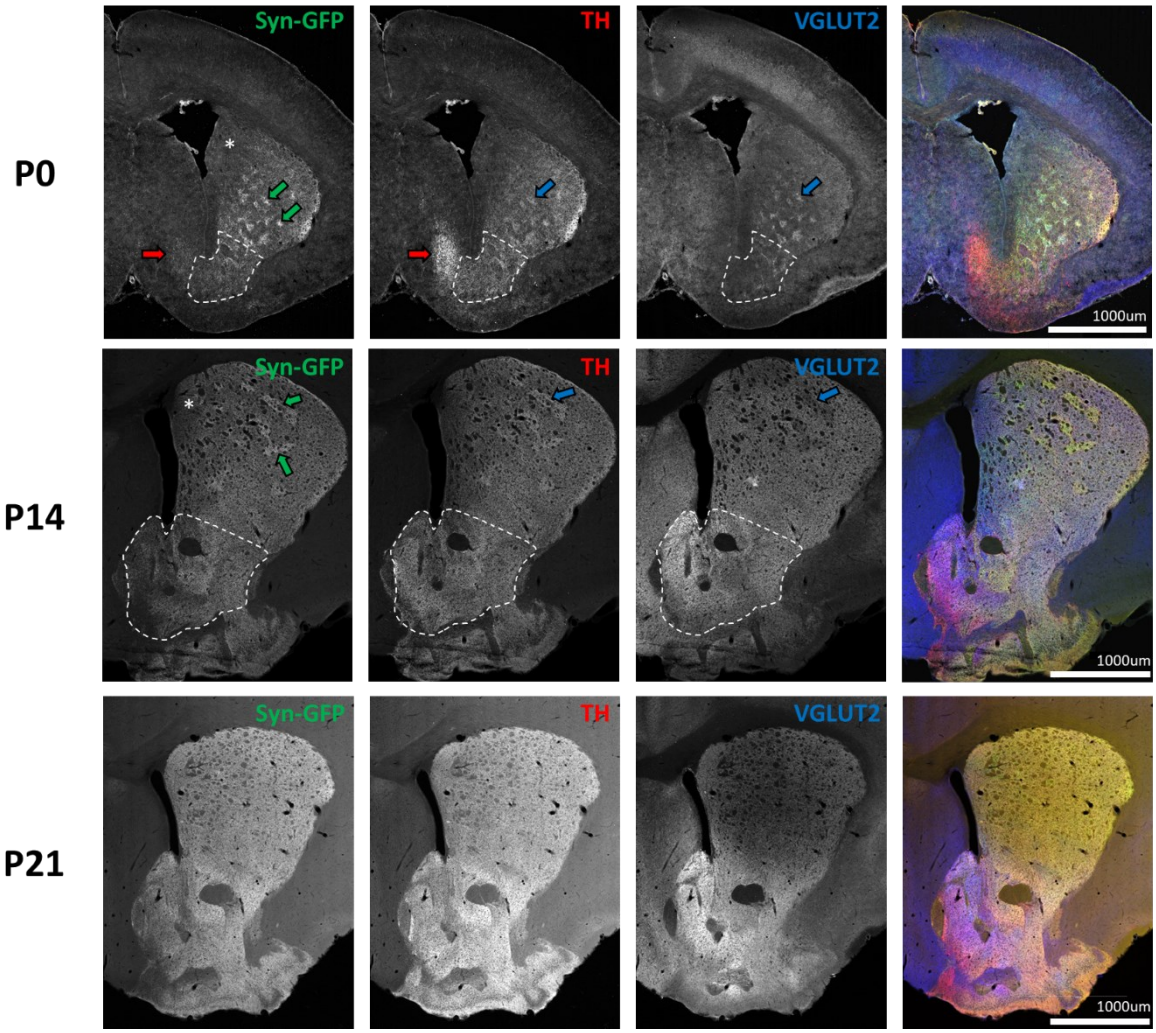

Figure 6. Representative images of the striatum at P0, P14, and P21 of Dat-Cre/Th-Flp/FPSiT mice, taken using confocal microscopy. Syn-GFP in green, TH in red, and VGLUT2 in blue. Patches of Syn-GFP in the striatum are visible at P0 and P14 (green arrows). TH is denser in these patches compared to surrounding matrix at P0 and P14, whereas VGLUT2 is only denser in patches at P0 (blue arrows). Expression of TH, but not Syn-GFP, is visible in an area ventromedial to the striatum at P0 (red arrows). The NAc is not visually defined by DAergic or glutamatergic innervation at P0, but by P14 the NAc is visually defined, with dense glutamatergic innervation of the medial shell (white dotted outlines). The dorsomedial shell is not innervated by DAergic or glutamatergic projections at P0, whereas by P14 innervation is apparent (white asterisks).

The dorsomedial striatum receives DAergic and glutamatergic innervation after P0

At P0, one sample t-tests have revealed that the fluorescence intensity of Syn-GFP, TH, and VGLUT2 is not significantly different from background fluorescence intensity (Syn-GFP, p >

0.9; TH, $p > 0.7$; VGLUT2, $p > 0.5$; one sample t-tests, $n = 3$ for all groups) (Figure 7). This demonstrates the absence of DAergic and glutamatergic innervation in the dorsomedial striatum at birth. At P14, one sample t-tests show that the level of fluorescence intensity in the dorsomedial striatum is greater than background in all three channels (Syn-GFP, $p < 0.02$; TH, $p < 0.03$; VGLUT2, $p < 0.5$; one sample t-tests, $n = 4$ for all groups) (Figure 7). This demonstrates that DAergic and glutamatergic innervation of the dorsomedial striatum takes place postnatally.

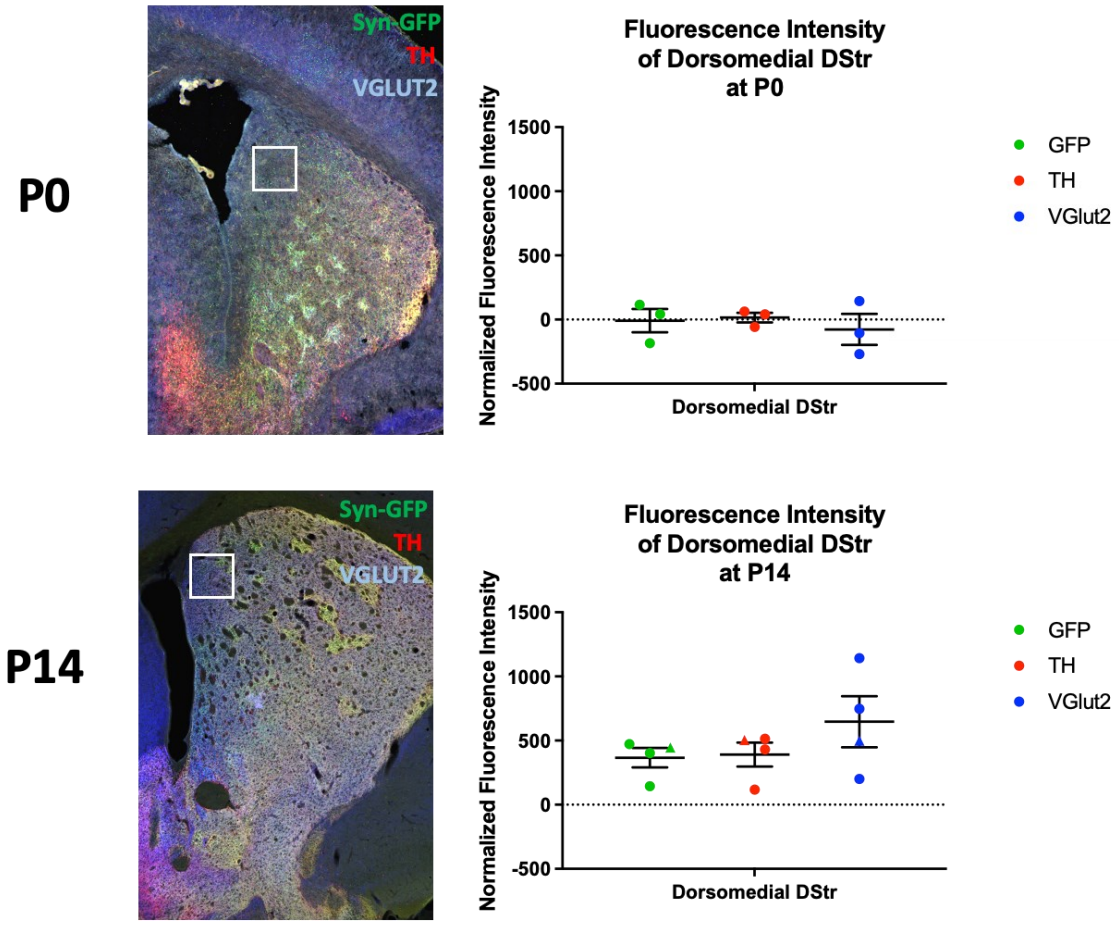

Figure 7. Fluorescence intensity analysis of DAergic and glutamatergic innervation of the dorsomedial aspect of the dorsal striatum (DStr) at P0 and P14. Confocal images of the striatum were taken after immunofluorescence staining of GFP, TH, and VGLUT2. White squares represent ROI used to measure mean fluorescence intensity within the dorsomedial striatum at P0 and P14. Fluorescence intensity has been normalized to background fluorescence of the tissue. The results of fluorescence intensity analysis demonstrate that DAergic and glutamatergic innervation of the dorsomedial striatum increases postnatally. Data represented as mean +/- SEM. Circles denote males, triangles denote females.

DAergic and glutamatergic innervation of the NAc at P14 varies between the core and shell

To investigate how the NAc is innervated at P14, four locations within the NAc were selected for fluorescence intensity analysis: the core, the lateral shell, the ventral shell, and the dorsomedial shell (Figure 8).

Fluorescence intensity of Syn-GFP is significantly different between at least three locations in the NAc (Figure 8, n = 4, $F(2.694, 8.081) = 12.0$, $P < 0.003$, repeated measures one-way ANOVA). Post-hoc Tukey's tests revealed that the fluorescence intensity of Syn-GFP is significantly lower in the NAc dorsomedial shell compared to both the lateral shell (adjusted p-value < 0.05) and the core (adjusted p-value < 0.04).

Fluorescence intensity of TH and VGLUT2 are not statistically different across NAc locations based on ANOVA testing (Figure 8, n=4 for all groups, TH: $F(1.268, 3.804) = 4.7$, $P > 0.09$; VGLUT2: $F(1.017, 3.050) = 5.6$, $P > 0.09$, repeated measures one-way ANOVA). However, post-hoc Tukey's tests revealed that the fluorescence intensity of TH is significantly lower in the NAc dorsomedial shell compared to the NAc core (adjusted p-value < 0.002), which matches the pattern of Syn-GFP fluorescence intensity. Post-hoc Tukey's tests did not find any significant differences in VGLUT2 fluorescence intensity across the NAc, though there appears to be a trend for greater density of VGLUT2 in the NAc dorsomedial shell compared to the rest of the NAc (Figure 8).

Altogether, these results demonstrate that DAergic innervation of the NAc is denser in the core of the NAc compared to the dorsomedial shell, and a non-significant trend in the data suggests that the opposite pattern is seen in glutamatergic innervation.

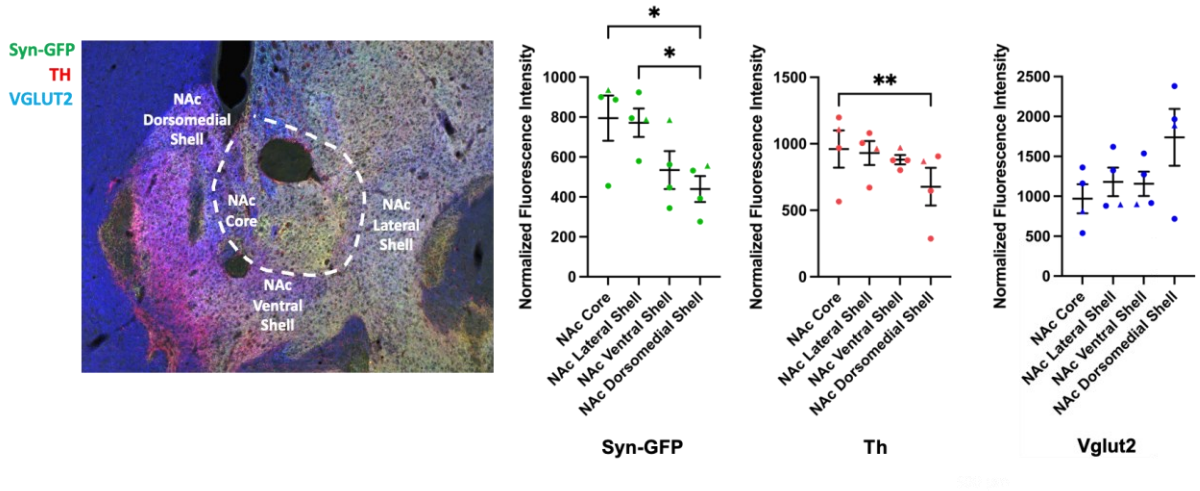

Figure 8. Fluorescence intensity analysis of DAergic and glutamatergic innervation of four locations within the NAc at P14. Confocal images of the NAc were taken after immunofluorescence staining of GFP, TH, and VGLUT2. The perimeter of the NAc core is traced with a white dotted outline, and text labels are placed in corresponding locations of the lateral shell, ventral shell, and dorsomedial shell. Fluorescence intensity has been normalized to background fluorescence of the tissue. Data represented as mean +/- SEM. * $p < 0.05$, ** $p < 0.01$. Circles denote males, triangles denote females.

DAergic innervation of the striatum at P0 and P14 is denser in patches compared to matrix, whereas glutamatergic innervation is denser in patches at P0 and not at P14

To study the patch-and-matrix organization of DAergic and glutamatergic innervation in the striatum in early postnatal development, four rostral-caudal levels were selected for analysis (L1-L4) (Figure 3). L1-L3 was analyzed at P0, and L1-L4 was analyzed at P14 (Figure 9). L4 was not analyzed at P0 due to inconsistent tissue quality.

There is a significant difference in fluorescence intensity of Syn-GFP between patches and matrix of the striatum at P0 ($F(1,3) = 32.6$, $P < 0.02$, mixed-effects analysis). Post-hoc Bonferroni tests reveal that, in rostral-caudal levels L1 and L2, the fluorescence intensity of Syn-GFP is greater in patches compared to matrix (Figure 9, L1: n = 4, adjusted p-value < 0.02; L2: n = 4, adjusted p-value < 0.05). This difference is not statistically significant in L3 (Figure 9, L3: n = 3,

adjusted p-value > 0.2). This same pattern is also seen in fluorescence intensity of TH. There is a significant difference in TH fluorescence intensity between patches and matrix ($F(1,3) = 24.7$, $P < 0.02$, mixed-effects analysis). More specifically, TH fluorescence intensity is greater in patches compared to matrix in L1 and L2 but not in L3 (Figure 9, L1: n = 4, adjusted p-value < 0.05; L2: n = 4, adjusted p-value < 0.05; L3: n = 3, adjusted p-value > 0.2). The fluorescence intensity of VGLUT2 is significantly different between patches and matrix ($F(1,3) = 26.0$, $P < 0.02$, mixed-effects analysis) and post-hoc Bonferroni tests reveal that VGLUT2 fluorescence is greater in patches compared to matrix at L1 with statistical significance (Figure 9, L1: n = 4, adjusted p-value < 0.04) and a trend can be seen for greater VGLUT2 fluorescence intensity in patches at L2, though not statistically significant (Figure 9, L2: n = 4, adjusted p-value < 0.06). Altogether, these results demonstrate that DAergic innervation (including the presence of release sites) is greatest in patches of the striatum at P0, more prominently in the rostral areas of the striatum, and that glutamatergic innervation is also present in these patches in the rostral striatum.

At P14, the fluorescence intensity of Syn-GFP is significantly different in patches versus matrix ($F(1,3) = 112.5$, $P < 0.002$, mixed-effects analysis) and post-hoc Bonferroni tests reveal that Syn-GFP fluorescence intensity is greater in patches compared to matrix in all levels of the striatum except for L1 (Figure 9, L1: n = 3, adjusted p-value > 0.1; L2: n = 4, adjusted p-value < 0.02; L3: n = 4, adjusted p-value < 0.04; L4: n = 4, adjusted p-value < 0.003). This pattern is also seen in TH fluorescence intensity, which is significantly different in patches versus matrix ($F(1,3) = 80.5$, $P < 0.003$, mixed-effects analysis). More specifically, TH fluorescence intensity is greater in patches compared to matrix for all levels of the striatum except for L1 (Figure 9, L1: n = 3, adjusted p-value > 0.6; L2: n = 4, adjusted p-value < 0.0006; L3: n = 4, adjusted p-value < 0.04; L4: n = 4, adjusted p-value < 0.02). The fluorescence intensity of VGLUT2 is not statistically

different between patches and matrix across all levels of the striatum ($F(1,3) = 4.4$, $P > 0.1$, mixed-effects analysis). Overall, these results demonstrate that patches of DAergic innervation are conserved at P14, though glutamatergic innervation in the striatum at this timepoint is no longer concentrated within patches.

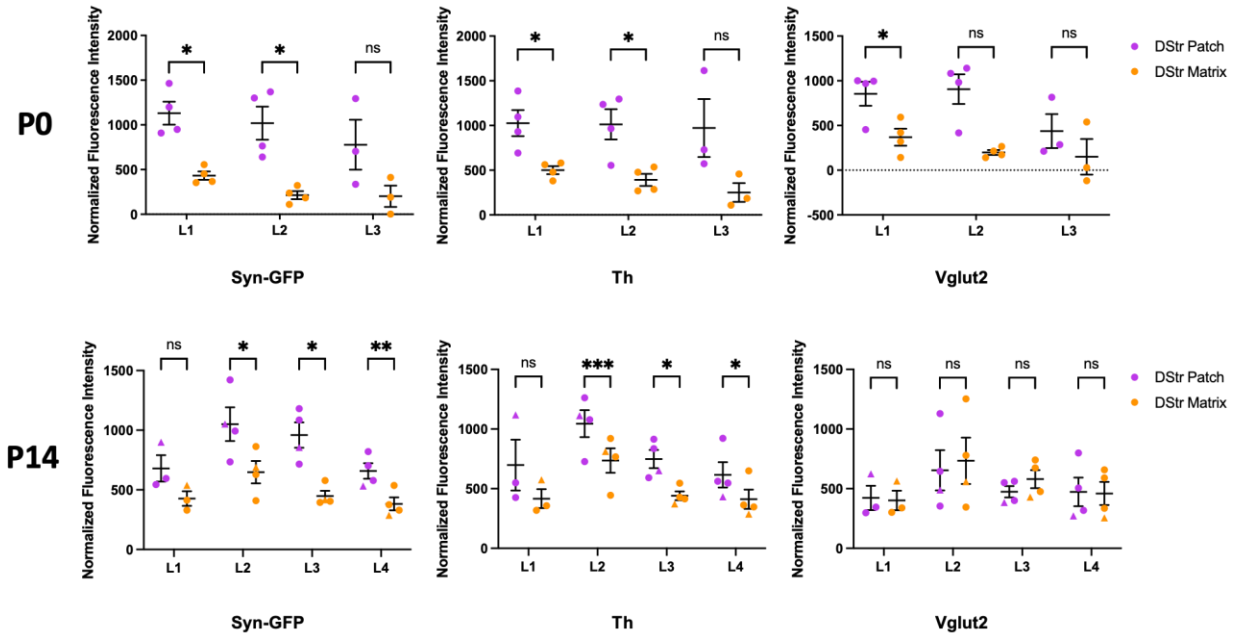

Figure 9. Fluorescence intensity analysis of DAergic and glutamatergic innervation in patches and matrix of the striatum across three rostral-caudal levels (L1-L3) at P0 and four rostral-caudal levels (L1-L4) at P14. DAergic innervation in the striatum is denser in patches compared to matrix at P0 and P14, whereas glutamatergic innervation is only denser in patches of the rostral striatum at P0. Fluorescence intensity has been normalized to background fluorescence of the tissue. Data represented as mean +/- SEM. * $p < 0.05$, ** $p < 0.01$, ns, not significant. Circles denote males, triangles denote females.

No significant difference in pattern of DAergic or glutamatergic innervation in the striatum at P0 or P14 in SHANK3b mutant mice

To investigate whether structural DAergic or glutamatergic circuit development is altered in a mouse model of ASD, Dat-Cre/Th-Flp/FPSiT mice were crossed with SHANK3b mutant mice to generate Dat-Cre/Th-Flp/FPSiT/SHANK3b mutant mice, then the same triple immunofluorescence procedure (staining for Syn-GFP, TH, and VGLUT2) was performed on

striatal sections from these mice at P0 and P14. Fluorescence intensity analysis was then performed to compare striatal development in SHANK3b mutant mice with wildtype controls.

At P0, no significant differences were found in Syn-GFP fluorescence intensity between patches or matrix of the striatum in Dat-Cre/Th-Flp/FPSiT mice compared to Dat-Cre/Th-Flp/FPSiT/SHANK3b mutant mice across all levels (Patches: $F(1,6) = 0.1$, $P > 0.7$, mixed-effects analysis, non-significant effect of genotype; Matrix: $F(1,6) = 1.6$, $P > 0.2$, mixed-effects analysis, non-significant effect of genotype). Similarly, no significant differences were found in TH or VGLUT2 fluorescence intensity between patches or matrix of the striatum in Dat-Cre/Th-Flp/FPSiT mice compared to Dat-Cre/Th-Flp/FPSiT/SHANK3b mutant mice across all levels (Patches TH: $F(1,6) = 0.1$, $P > 0.7$; Matrix TH: $F(1,6) = 0.4$, $P > 0.5$; Patches VGLUT2: $F(1,6) = 0.3$, $P > 0.6$; Matrix VGLUT2: $F(1,6) = 0.1$, $P > 0.7$; mixed-effects analysis, non-significant effect of genotype).

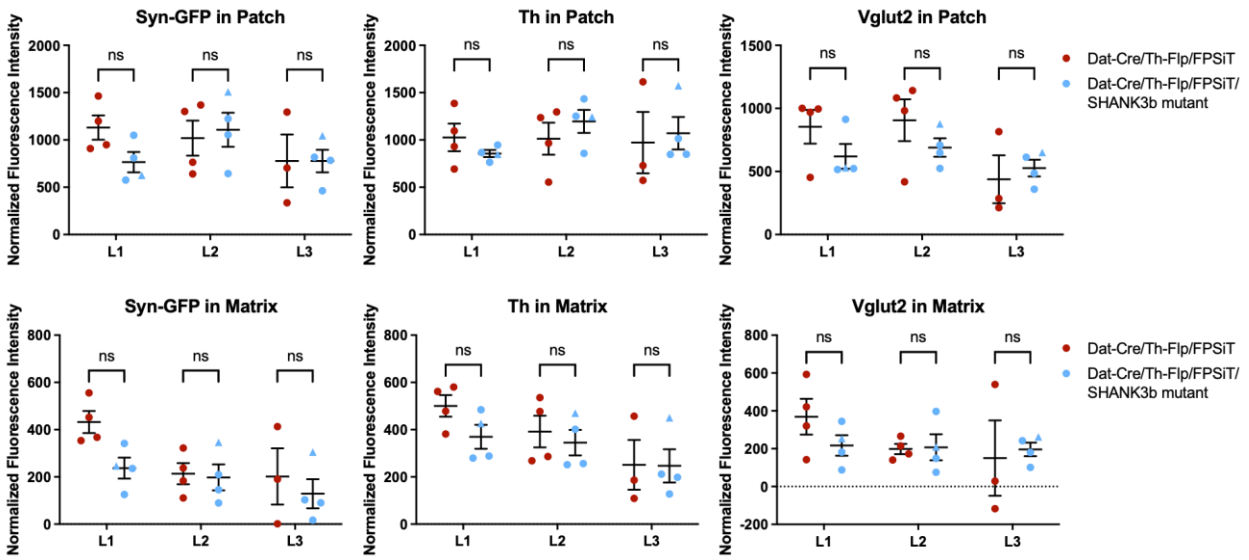

Figure 10. Fluorescence intensity analysis of DAergic and glutamatergic innervation in patches and matrix of the striatum across three rostral caudal levels (L1-L3) at P0 in Dat-Cre/Th-Flp/FPSiT mice compared to Dat-Cre/Th-Flp/FPSiT/SHANK3b mutant mice. DAergic and glutamatergic innervation in the striatum of SHANK3b mutant mice does not significantly differ from control. Fluorescence intensity has been normalized to background fluorescence of the tissue. Data represented as mean +/- SEM. ns, not significant. Circles denote males, triangles denote females.

At P14, no significant differences were found in Syn-GFP fluorescence intensity between patches or matrix of the striatum in Dat-Cre/Th-Flp/FPSiT mice compared to Dat-Cre/Th-Flp/FPSiT/SHANK3b mutant mice across all levels (Patches: $F(1,6) = 0.3$, $P > 0.6$, mixed-effects analysis, non-significant effect of genotype; Matrix: $F(1,6) = 1.6$, $P > 0.2$, mixed-effects analysis, non-significant effect of genotype). Similarly, no significant differences were found in TH or VGLUT2 fluorescence intensity between patches or matrix of the striatum in Dat-Cre/Th-Flp/FPSiT mice compared to Dat-Cre/Th-Flp/FPSiT/SHANK3b mutant mice across all levels (Patches TH: $F(1,6) = 0.9$, $P > 0.3$; Matrix TH: $F(1,6) = 0.006$, $P > 0.9$; Patches VGLUT2: $F(1,6) = 0.6$, $P > 0.4$; Matrix VGLUT2: $F(1,6) = 0.02$, $P > 0.8$; mixed-effects analysis, non-significant effect of genotype).

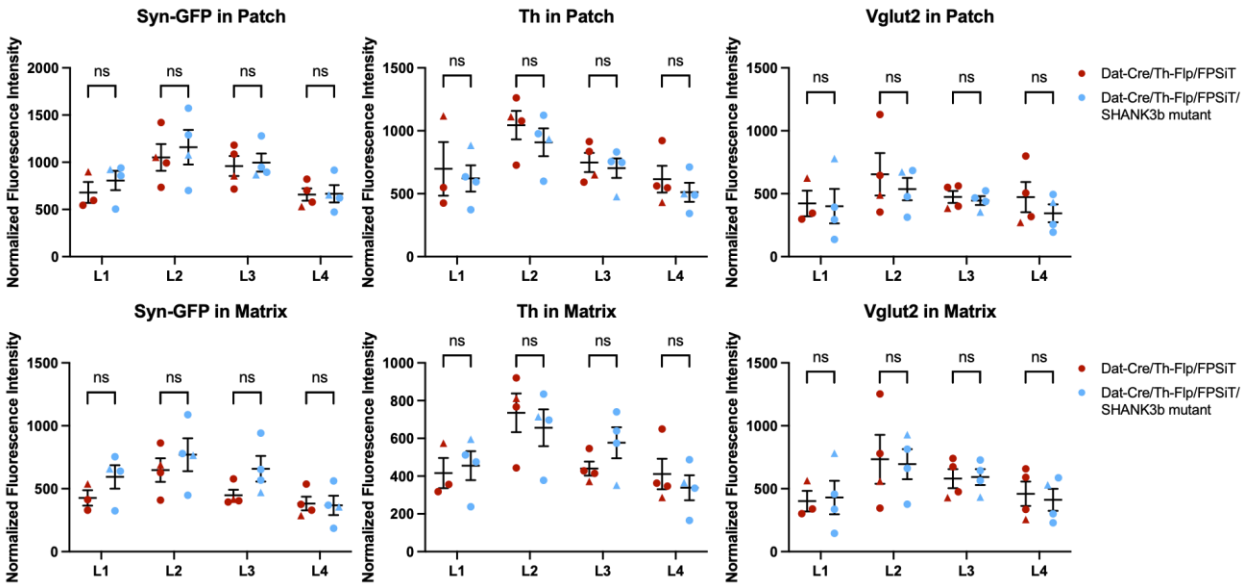

Figure 11. Fluorescence intensity analysis of DAergic and glutamatergic innervation in patches and matrix of the striatum across four rostral caudal levels (L1-L4) at P14 in Dat-Cre/Th-Flp/FPSiT mice compared to Dat-Cre/Th-Flp/FPSiT/SHANK3b mutant mice. DAergic and glutamatergic innervation in the striatum of SHANK3b mutant mice does not significantly differ from control. Fluorescence intensity has been normalized to background fluorescence of the tissue. Data represented as mean +/- SEM. ns, not significant. Circles denote males, triangles denote females.

Fluorescence intensity of Syn-GFP, TH, and VGLUT2 has been analyzed and compared across the different areas of the NAc (Figure 12). There are no significant differences in fluorescence intensity of Syn-GFP across the structures of the NAc in Dat-Cre/Th-Flp/FPSiT mice compared to Dat-Cre/Th-Flp/FPSiT/SHANK3b mutant mice ($F(1,6) = 2.2$, $P > 0.1$, two-way ANOVA, non-significant effect of genotype). Similarly, no significant differences were found in fluorescence intensity of TH or VGLUT2 across the NAc in Dat-Cre/Th-Flp/FPSiT mice compared to Dat-Cre/Th-Flp/FPSiT/SHANK3b mutant mice (TH: $F(1,6) = 0.5$, $P > 0.5$; VGLUT2: $F(1,6) = 0.7$, $P > 0.4$; two-way ANOVA, non-significant effect of genotype).

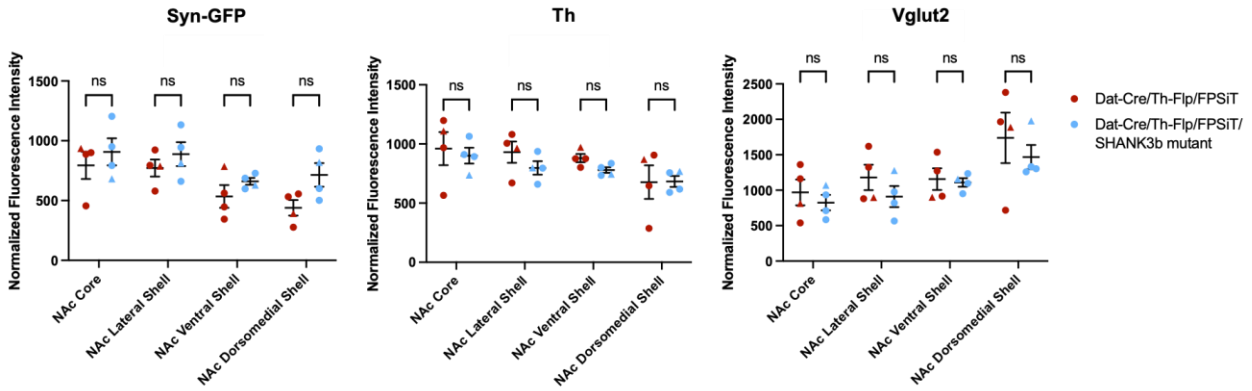

Figure 12. Fluorescence intensity analysis of DAergic and glutamatergic innervation in four locations within the NAc at P14 in Dat-Cre/Th-Flp/FPSiT mice compared to Dat-Cre/Th-Flp/FPSiT/SHANK3b mutant mice. DAergic and glutamatergic innervation of the NAc at P14 in SHANK3b mutant mice does not significantly differ from control. Fluorescence intensity has been normalized to background fluorescence of the tissue. Data represented as mean +/- SEM. ns, not significant. Circles denote males, triangles denote females.

Overall, these results demonstrate that the structural development of DAergic and glutamatergic circuits into the striatum during early postnatal development is very similar between wildtype and SHANK3b mutant mice.

Discussion

The aim of this project was to establish the pattern of development of DAergic and glutamatergic circuits in the striatum of mice and to investigate whether this development is altered in a mouse model of ASD. The results show that, in typical neurodevelopment, putative release sites of neurotransmitters on DAergic projections in the striatum concentrate in patches at birth and through the first two weeks of life, and then become more diffusely spread in the striatum by three weeks of life. Glutamatergic innervation spreads outside of patches sooner than DAergic innervation, by two weeks of age. DAergic and glutamatergic innervation of the striatum develops ventrolaterally to dorsomedially from birth to two weeks of age, as evidenced by the delayed innervation of the dorsomedial striatum. Additionally, the core and shell of the NAc become defined by DAergic and glutamatergic innervation by two weeks of age. DAergic innervation of the NAc is higher in the core compared to the dorsomedial shell at P14, opposite to a non-significant trend seen in glutamatergic innervation. In SHANK3b mutant mice, the results of behavioural testing show that SHANK3b mutant mice demonstrate a reduction in social behaviour compared to control mice, which is an ASD-like symptom of this strain. Analysis of the striatum in SHANK3b mutant mice has shown no significant differences in DAergic or glutamatergic striatal circuit development between SHANK3b mutant mice and control mice in early postnatal development, though the future directions of this research aim to investigate whether there are specific structural or functional differences in DAergic circuits in SHANK3b mutant mice.

A common technique for axonal tracing in mice is to inject an adeno-associated virus (AAV) into the brain region of interest via stereotaxic surgery, then wait several weeks for maximal virus expression before euthanizing and examining the brain (Nectow & Nestler, 2020). The use of RC::FPSiT mice in this study allows the labelling of DAergic neural projections without

the need to perform an AAV injection. This is an advantage because AAV injection relies on accurate and reproducible virus targeting, which is time-consuming and can be difficult especially in very young animals. By contrast, early postnatal RC::FPSiT mice can be euthanized and examined without any prior procedure.

This study relies on the use of synaptophysin to identify release sites of neurotransmitters from DAergic projections, based on the knowledge that synaptophysin is a synaptic vesicle protein and synaptic vesicles typically localize to active zones where neurotransmitters are released (Valtorta et al., 2004). However, two important notes must be made here. First, it is important to note that DA release in the striatum first occurs between P6 and P10 (Kim et al., 2002) and DA release was not measured in this study. Thus, the results discussed for circuit development at P0 are limited to the structural capacity for neurotransmitter release in developing DAergic neurons. As such, the results demonstrate that putative release sites of neurotransmitters on DAergic projections are present at least 6 days before DA release is expected to first occur. This is supported by previous research which has shown that VMAT2, a presynaptic protein located on synaptic vesicles which is required for DA transmission, is detectable in the striatum by P1 in rats (Leroux-Nicollet et al., 1990). Second, it has been found that roughly 30% of DA varicosities contain the necessary active zone proteins for neurotransmitter release, such as regulating synaptic membrane exocytosis 1 (RIM1) (Liu et al., 2018). Since the current study did not confirm whether RIM1 was present at release sites, the results discussed here pertain only to putative release sites of neurotransmitters in the striatum. Further research should be conducted to elucidate whether the distribution of active release sites differs from the results reported presently.

Additionally, several subtypes of DA neurons exist which co-transmit neurotransmitters other than DA (Poulin et al., 2020). Since Syn-GFP localizes to all neurotransmitter release sites

on DAergic neurons regardless of which neurotransmitter is released at a particular site, then Syn-GFP in this study indicates the presence of putative release sites, but not strictly DA release sites, on DAergic projections.

DAergic and glutamatergic innervation of the striatum develops in a patch-and-matrix pattern

Previous literature has used TH or DA immunolabeling to visualize early post-natal DAergic circuit development in the striatum (Antonopoulos et al., 2002; Fentress et al., 1981; Voorn et al., 1988). The results of the current study agree with previous research which has also demonstrated that DAergic innervation into patches of the striatum is denser than innervation into the matrix during early postnatal development. However, previous literature did not specifically visualize putative release sites on DAergic projections. As such, this study adds to the current body of knowledge by demonstrating that the distribution of release sites on DAergic projections is highly concentrated in patches. This has implications for where neurotransmitter release from DA neurons might first occur in the striatum.

Conflicting evidence has been presented on whether DA release is greater in patches or matrix of the striatum in adulthood (Brimblecombe & Cragg, 2016). Research in rats has shown that the distribution of DAergic projections in the striatum is denser in patches, suggesting greater DA transmission (Matsuda et al., 2009) whereas research in humans has shown via immunolabeling that the concentration of TH is denser in the matrix of the caudate and putamen (the human equivalent of the rodent striatum) (Morigaki & Goto, 2016). Although the results of the current study focus on patches in development and not adulthood, it is informative to know that release sites on DAergic neurons remain concentrated in patches after dopamine release has begun, which suggests that neurotransmitter release from DA neurons might be higher in patches during development in mice.

Another finding of the current study is that VGLUT2 is concentrated in patches at P0. It has been shown previously that VGLUT2 is densely present in patches of the DStr at P0, and then becomes slightly more dense in the matrix after P10 (Nakamura et al., 2005), which supports the findings of the current study. In embryonic development (E11.5), nearly all DAergic midbrain neurons express VGLUT2, but by E14.5, expression of VGLUT2 is no longer detectable in lateral regions of the mesencephalon (embryonic midbrain), which indicates that downregulation of VGLUT2 expression in DAergic neurons outside of the VTA occurs before birth (Kouwenhoven et al., 2020). In embryonic development of mice, midbrain DAergic neurons from the SNc and VTA send nonspecific projections into both the DStr and VStr, but by birth, the pathways from the SNc to the DStr and the VTA to the VStr have differentiated into separate pathways via axonal pruning (Hu et al., 2004). Taken together, these studies indicate that the source of VGLUT2 in patches of the striatum is not from DAergic neurons; rather, this is likely glutamatergic innervation from the thalamus, which innervates the striatum in adulthood (Fujiyama et al., 2004).

DAergic and glutamatergic innervation of the striatum spreads dorsomedially

It was found that the dorsomedial striatum does not receive DAergic and glutamatergic innervation at P0, whereas at P14, the dorsomedial striatum does receive DAergic and glutamatergic innervation. This implies that DAergic and glutamatergic innervation of the striatum spreads dorsomedially during postnatal development. This finding is supported by previous research which demonstrated that DAergic innervation into the striatum follows a ventrolateral to dorsomedial gradient in rats (Voorn et al., 1988), and demonstrates that this same pattern is found in mice.

The NAc receives differential innervation from DAergic and glutamatergic afferents

Innervation of the NAc at P14 showed that DAergic innervation was the least dense in the dorsomedial shell of the NAc, and glutamatergic innervation showed the opposite pattern. Previous research has shown that VGLUT2+ DA neurons of the VTA project exclusively to the medial shell of the NAc in adulthood (Poulin et al., 2018). Furthermore, VGLUT2+ DA neurons are the only midbrain DAergic neurons that send projections to the dorsomedial shell of the NAc, while other DA neurons project to the DStr and other areas of the NAc (Mingote et al., 2019). Axonal pruning during embryonic development results in the separation of SNc to DStr and VTA to VStr pathways (Hu et al., 2004). This information taken together with the results of the current study suggests that the distribution of DAergic release sites in the dorsomedial striatum at P14 are exclusively from VGLUT2+ DAergic neurons from the VTA.

SHANK3b mutant mice do not demonstrate a social preference in the modified 3-chamber sociability test

To validate the phenotype of the ASD model (SHANK3b mutant), the 3-chamber sociability test was used. The format of the 3-chamber sociability test varies between studies, which may be a contributing factor in the variability of results reported in the literature regarding social deficits in mouse models of ASD (Bukatova et al., 2021). The optimized version of this test for use with mouse models of ASD (Rein et al., 2020) aims to reduce this variability by including an additional phase where the mouse is familiarized with the presence of objects (paper towel balls) within the chambers before being given the choice to investigate a novel object versus a social target. The results of the 3-chamber sociability test shows that SHANK3b mutant mice do not prefer to interact with a social stimulus compared to a non-social stimulus, which is expected based on previous research (Balaan et al., 2019; Peça et al., 2011) and suggests they may

experience less feelings of reward in response to social behaviour. This would result in lower social motivation, thus reducing the time spent interacting with the social target compared to control mice.

DAergic and glutamatergic circuit development does not significantly differ between SHANK3b mutant mice and control mice

This study did not find significant differences in striatal DAergic or glutamatergic circuit development at P0 or P14 between SHANK3b mutant mice and control mice. These results can inform us about the general spatial distribution of DAergic projections and release sites but do not provide more specific information such as the identity of release sites, the release properties of these sites, or the broader functional properties of these neurons during development in SHANK3b mutant mice. There may be subtype-specific differences in DAergic neural circuits in SHANK3b mutant mice which were not detected in this study. For example, in VGLUT2+ DA neurons, it is possible that glutamate release sites are particularly affected in SHANK3b mutant mice, even though the overall development of these neurons does not appear different from control. It has been reported that MSNs regulate the segregation of DAergic and glutamatergic release sites on VGLUT2+ DA neurons (Fortin et al., 2019). It is possible, then, that the mutation of *Shank3* disrupts this effect, rendering MSNs ineffective in properly segregating release sites on DAergic neurons. Further research is required to determine whether there are release site-specific changes in the DAergic circuits of SHANK3b mutant mice.

Recent research has shown that patches of the striatum occupy a larger area in adulthood in a SHANK3 mutant mouse (exon 11 deletion) compared to SHANK3 wildtype mice, which may play a role in overgrooming (Ferhat et al., 2023). SHANK3b mutant mice are also known to overgroom (Peca et al., 2012). It would be interesting to analyze striosome size in SHANK3b

mutant mice to determine whether these results are supported across different SHANK3 mutant models. Additionally, Ferhat et al. (2023) did not analyze patch size in early development. It is possible, then, that the area of DAergic and glutamatergic innervation in the striatum during development is larger in SHANK3b mutant mice compared to wildtype mice, despite the finding that the density of these projections is not significantly altered.

Limitations

This study has several limitations which must be discussed. For the 3-chamber sociability test, littermates were not exclusively used as controls, and the sample sizes for both the control and experimental groups were lower than what is typically required for sufficient statistical power (Silverman et al., 2010). Additionally, mixed sexes were used in both groups, and some ASD models (such as SHANK3 +/ΔC mice, in which the *Shank3* gene mutation results in deletion of the C-terminal region of the SHANK3 protein) display a sex-specific behavioural phenotype in the 3-chamber sociability assay (Rein et al., 2020). Another important caveat to the behavioural testing reported here is that the mice had undergone an invasive procedure including placement of a chronic intracranial implant prior to being used for behavioural testing. This likely caused additional stress in these mice, which may have exacerbated the behavioural phenotype in SHANK3b mutant mice. Despite these limitations, the results of the 3-chamber sociability test reported here are supported by previous research using this mouse model, and other SHANK3-deficient mouse models (Balaan et al., 2019; Peça et al., 2011; Rein et al., 2020).

In the fluorescence analysis of the NAc in Dat-Cre/Th-Flp/FPSiT mice, we observed a significant variability in the VGLUT2 data for the dorsomedial shell of the NAc (Figure 8). It is possible that this is the reason why a statistical difference was not found between the fluorescence intensity of the dorsomedial shell and the other regions of the NAc. Due to the small sample size,

the statistical power wasn't high enough to confirm the trend seen in the data. The same limitation (small sample size) applies to both the Dat-Cre/Th-Flp/FPSiT and Dat-Cre/Th-Flp/FPSiT/SHANK3b mutant groups used for fluorescence analysis in this study.

Future directions

Future directions include a functional analysis of the activity of the mesolimbic DA pathway during social interaction in SHANK3b mutant mice. To date, no publication has investigated *in vivo* DA activity in the mesolimbic pathway during social interaction in mouse models of ASD. This will be a highly informative study to elucidate how social stimuli is encoded in the DAergic reward pathway of the brain in a mouse model of ASD. Our lab is currently working on this project using fiber photometry to measure population activity of DAergic projections from the VTA to the medial shell of the NAc via *in vivo* calcium signaling using a stereotaxic virus injection (AAV-CAG-FLEX-jGCaMP8f) in Dat-Cre and Dat-Cre/SHANK3b mice. Our hypothesis is that there is reduced activity in the mesolimbic pathway in Dat-Cre/SHANK3b mutant mice during social interaction, reflecting less feelings of reward from social interaction as postulated in the DA hypothesis of ASD (Pavăl, 2017). The results obtained from this experiment will provide strong correlational evidence of DA circuit involvement in social interaction.

Additionally, it would be informative to look at the functional aspect of VGLUT2+ DA neurons specifically. As mentioned, the VTA is made up of mostly VGLUT2+ DA neurons which predominantly project to the medial shell of the NAc, forming part of the mesolimbic pathway which is thought to be involved in social behaviour (Gunaydin et al., 2014; Poulin et al., 2020). To investigate this, we are currently using VGLUT2-Cre/Dat-Flp mice with two adeno-associated viruses injected into the VTA (one that is Cre-OFF Flp-ON to target non-VGLUT2-expressing DAergic neurons, and the other that is Cre-ON Flp-ON to target specifically VGLUT2+ DA

neurons) combined with dual-channel fiber photometry such that the activity of both VGLUT2+ and VGLUT2- DA neurons can be recorded simultaneously during a social behaviour task. An interesting avenue to pursue would be to use optogenetics to selectively activate or inhibit the VGLUT2+ DA neurons of the VTA and investigate changes in social behaviour – we expect that social behaviour will be increased when VGLUT2+ DA neurons are activated, and reduced when VGLUT2+ DA neurons are inhibited. If our hypotheses are correct, the results of this experiment will provide strong support for the role of VGLUT2+ DA neurons in social behaviour, which can inform future research on how this specific subtype may be altered in ASD.

Conclusions

This study aimed to characterize the early postnatal development of striatal DAergic and glutamatergic circuits in mice, with a focus on the distribution of release sites on DAergic projections, and to compare how this development may be altered in a mouse model of ASD. These aims were achieved using an intersectional genetic model (Dat-Cre/Th-Flp/FPSiT) which allows visualization of release sites on DAergic neurons in the striatum through expression of Syn-GFP, and SHANK3b mutant mice which is a mouse model of ASD. Triple immunofluorescence (Syn-GFP, TH, VGLUT2) was used to investigate the pattern of circuit development at birth (P0) and at two weeks of age (P14) in wildtype versus SHANK3b mutant mice. The results of this study demonstrate the patch-and-matrix pattern of DAergic circuit development in the striatum, which is supported by previous literature, and adds new evidence for the presence of neurotransmitter release sites on DAergic projections within patches, which suggests that neurotransmitter release from DAergic neurons in the striatum may be higher in patches compared to the matrix in early postnatal development. Innervation of the dorsomedial striatum occurs postnatally, which suggests that DAergic and glutamatergic innervation begins ventrolaterally in the striatum and spreads dorsomedially as the striatum develops. Additionally, the NAc becomes defined by DAergic and glutamatergic innervation by two weeks of age, and the dorsomedial shell of the NAc is innervated by VGLUT2+ DA neurons by this timepoint. SHANK3b mutant mice demonstrate non-social preference as evidenced by the 3-chamber sociability test, which supports the behavioural phenotype of this mouse model. The density of DAergic and glutamatergic innervation of the striatum at birth and two weeks of age does not significantly differ between SHANK3b mutant mice and wildtype controls. Future directions are recommended to fully elucidate the role of DA circuit development and function in ASD.

References

American Psychiatric Association. (2013). *Diagnostic and Statistical Manual of Mental Disorders*. https://doi.org/10.1176/APPI.BOOKS.9780890425596

Antonopoulos, J., Dori, I., Dinopoulos, A., Chiotelli, M., & Parnavelas, J. G. (2002). Postnatal development of the dopaminergic system of the striatum in the rat. *Neuroscience*, *110*(2), 245–256. https://doi.org/10.1016/S0306-4522(01)00575-9

Arpi, M. N. T., & Simpson, T. I. (2022). SFARI genes and where to find them; modelling Autism Spectrum Disorder specific gene expression dysregulation with RNA-seq data. *Scientific Reports*, *12*(1), 1–15. https://doi.org/10.1038/s41598-022-14077-1

Ayano, G. (2016). Dopamine: Receptors, Functions, Synthesis, Pathways, Locations and Mental Disorders: Review of Literatures. *Journal of Mental Disorders and Treatment*, *2*(2). https://doi.org/10.4172/2471-271X.1000120

Bäckman, C. M., Malik, N., Zhang, Y. J., Shan, L., Grinberg, A., Hoffer, B. J., Westphal, H., & Tomac, A. C. (2006). Characterization of a mouse strain expressing Cre recombinase from the 3′ untranslated region of the dopamine transporter locus. *Genesis (United States)*, *44*(8), 383–390. https://doi.org/10.1002/dvg.20228

Bai, X., & Strong, R. (2014). Expression of synaptophysin protein in different dopaminergic cell lines. *Journal of Biochemical and Pharmacological Research*, *2*(4), 185-190.

Balaan, C., Corley, M. J., Eulalio, T., Leite-ahyo, K., Pang, A. P. S., Fang, R., Khadka, V. S., Maunakea, A. K., & Ward, M. A. (2019). Juvenile Shank3B deficient mice present with behavioral phenotype relevant to autism spectrum disorder. *Behavioural Brain Research*, *356*, 137. https://doi.org/10.1016/J.BBR.2018.08.005

Baribeau, D. A., Dupuis, A., Paton, T. A., Hammill, C., Scherer, S. W., Schachar, R. J., Arnold, P. D., Szatmari, P., Nicolson, R., Georgiades, S., Crosbie, J., Brian, J., Iaboni, A., Kushki, A., Lerch, J. P., & Anagnostou, E. (2019). Structural neuroimaging correlates of social deficits are similar in autism spectrum disorder and attention-deficit/hyperactivity disorder: analysis from the POND Network. *Translational Psychiatry*, *9*(1). https://doi.org/10.1038/S41398-019-0382-0

Bariselli, S., Tzanoulinou, S., Glangetas, C., Prévost-Solié, C., Pucci, L., Viguié, J., Bezzi, P., O'Connor, E. C., Georges, F., Lüscher, C., & Bellone, C. (2016). SHANK3 controls maturation of social reward circuits in the VTA. *Nature Neuroscience*, *19*(7), 926–934. https://doi.org/10.1038/nn.4319

Best, J. A., Nijhout, H. F., & Reed, M. C. (2009). Homeostatic mechanisms in dopamine synthesis and release: a mathematical model. *Theoretical Biology & Medical Modelling*, *6*, 21. https://doi.org/10.1186/1742-4682-6-21

Boeckers, T. M. (2006). The postsynaptic density. *Cell and Tissue Research*, *326*(2), 409–422. https://doi.org/10.1007/s00441-006-0274-5

Bonnavion, P., Varin, C., Fakhfouri, G., Olondo, P. M., Groote, A. De, Cornil, A., Lopez, R. L., Fernandez, E. P., Isingrini, E., Rainer, Q., Xu, K., Tzavara, E., Vigneault, E., Dumas, S., d'Exaerde, A. de K., & Giros, B. (2023). Unexpected contributions of striatal projection neurons coexpressing dopamine D1 and D2 receptors in balancing motor control. *BioRxiv*. https://doi.org/10.1101/2022.04.05.487163

Brimblecombe, K. R., & Cragg, S. J. (2016). The Striosome and Matrix Compartments of the Striatum: A Path through the Labyrinth from Neurochemistry toward Function. *ACS Chem. Neurosci.,* 8(2), 235-242. https://doi.org/10.1021/acschemneuro.6b00333

Bukatova, S., Renczes, E., Reichova, A., Filo, J., Sadlonova, A., Mravec, B., Ostatnikova, D., Bakos, J., & Bacova, Z. (2021). Shank3 Deficiency is Associated With Altered Profile of Neurotransmission Markers in Pups and Adult Mice. *Neurochemical Research*, *46*(12), 3342–3355. https://doi.org/10.1007/S11064-021-03435-6/FIGURES/7

Chuhma, N., Mingote, S., Kalmbach, A., Yetnikoff, L., & Rayport, S. (2017). Heterogeneity in Dopamine Neuron Synaptic Actions Across the Striatum and Its Relevance for Schizophrenia. *Biological Psychiatry*, *81*(1), 43–51. https://doi.org/10.1016/J.BIOPSYCH.2016.07.002

Cox, J., & Witten, I. B. (2019). Striatal circuits for reward learning and decision-making. *Nature Reviews Neuroscience*, *20*(8), 482–494. https://doi.org/10.1038/s41583-019-0189-2

Dai, B., Sun, F., Tong, X., Ding, Y., Kuang, A., Osakada, T., Li, Y., & Lin, D. (2022). Responses and functions of dopamine in nucleus accumbens core during social behaviors. *Cell Reports*, *40*(8), 111246. https://doi.org/10.1016/j.celrep.2022.111246

Eskenazi, D., Malave, L., Mingote, S., Yetnikoff, L., Ztaou, S., Velicu, V., Rayport, S., & Chuhma, N. (2021). Dopamine Neurons That Cotransmit Glutamate, From Synapses to Circuits to Behavior. *Frontiers in Neural Circuits*, *15*, 40. https://doi.org/10.3389/fncir.2021.665386

Fentress, J. C., Stanfield, B. B., & Cowan, W. M. (1981). Observations on the development of the striatum in mice and rats. *Anatomy and Embryology*, *163*(3), 275–298. https://doi.org/10.1007/BF00315705

Fortin, G. M., Ducrot, C., Giguère, N., Kouwenhoven, W. M., Bourque, M.-J., Pacelli, C., Varaschin, R. K., Brill, M., Singh, S., Wiseman, P. W., & Trudeau, L. É. Segregation of dopamine and glutamate release sites in dopamine neuron axons: regulation by striatal target cells. *FASEB Journal*, *33*(1), 400–417. https://doi.org/10.1096/FJ.201800713RR

Fujiyama, F., Kuramoto, E., Okamoto, K., Hioki, H., Furata, T., Zhou, L., Nomura, S., & Kaneko, T. (2004). Presynaptic localization of an AMPA-type glutamate receptor in corticostriatal and thalamostriatal axon terminals. *European Journal of Neuroscience*, *20*, 3322–3330.

Gunaydin, L. A., Grosenick, L., Finkelstein, J. C., Kauvar, I. V., Fenno, L. E., Adhikari, A., Lammel, S., Mirzabekov, J. J., Airan, R. D., Zalocusky, K. A., Tye, K. M., Anikeeva, P., Malenka, R. C., & Deisseroth, K. (2014). Natural neural projection dynamics underlying social behavior. *Cell*, *157*(7), 1535–1551. https://doi.org/10.1016/j.cell.2014.05.017

Halladay, A. K., Bishop, S., Constantino, J. N., Daniels, A. M., Koenig, K., Palmer, K., Messinger, D., Pelphrey, K., Sanders, S. J., Singer, A. T., Taylor, J. L., & Szatmari, P. (2015). Sex and gender differences in autism spectrum disorder: summarizing evidence gaps and identifying emerging areas of priority. *Molecular Autism*, *6*(1). https://doi.org/10.1186/S13229-015-0019-Y

Hollander, E., Anagnostou, E., Chaplin, W., Esposito, K., Haznedar, M. M., Licalzi, E., Wasserman, S., Soorya, L., & Buchsbaum, M. (2005). Striatal volume on magnetic resonance imaging and repetitive behaviors in autism. *Biological Psychiatry*, *58*(3), 226–232. https://doi.org/10.1016/j.biopsych.2005.03.040

Hu, Z., Cooper, M., Crockett, D. P., & Zhou, R. (2004). Differentiation of the midbrain dopaminergic pathways during mouse development. *Journal of Comparative Neurology*, *476*(3), 301–311. https://doi.org/10.1002/cne.20230

Jimenez-Castellanos, J., & Graybiel, A. M. (1987). Subdivisions of the dopamine-containing A8-A9-A10 complex identified by their differential mesostriatal innervation of striosomes and extrastriosomal matrix. *Neuroscience*, *23*(1), 223–242. https://doi.org/10.1016/0306-4522(87)90285-5

Kandel, E. R., Schwartz, J. H., Jessell, T. M., Siegelbaum, S. A., & Hudspeth, A. J. (2013). *Principles of Neural Science* (5th ed.). The McGraw-Hill Companies.

Kim, D. S., Froelick, G. J., & Palmiter, R. D. (2002). Dopamine-dependent desensitization of dopaminergic signaling in the developing mouse striatum. *The Journal of Neuroscience*, *22*(22), 9841–9849. https://doi.org/10.1523/JNEUROSCI.22-22-09841.2002

Knowles, R., Dehorter, N., & Ellender, T. (2021). From Progenitors to Progeny: Shaping Striatal Circuit Development and Function. *The Journal of Neuroscience*, *41*(46), 9483–9502. https://doi.org/10.1523/JNEUROSCI.0620-21.2021

Kohls, G., Schulte-Rüther, M., Nehrkorn, B., Müller, K., Fink, G. R., Kamp-Becker, I., Herpertz-Dahlmann, B., Schultz, R. T., & Konrad, K. (2013). Reward system dysfunction in autism spectrum disorders. *Social Cognitive and Affective Neuroscience*, *8*(5), 565–572. https://doi.org/10.1093/scan/nss033

Kouwenhoven, W. M., Fortin, G., Penttinen, A.-M., Florence, C., Delignat-Lavaud, B., Bourque, M.-J., Trimbuch, T., Luppi, M. P., Salvail-Lacoste, A., Legault, P., Poulin, J.-F., Rosenmund, C., Awatramani, R., & Trudeau, L.-É. (2020). VGluT2 Expression in Dopamine Neurons Contributes to Postlesional Striatal Reinnervation. *The Journal of Neuroscience*, *40*(43), 8262–8275. https://doi.org/10.1523/JNEUROSCI.0823-20.2020

Kramer, D. J., Kosillo, P., Friedmann, D., Stafford, D., Luo, L., Yiu-Fai Lee, A., Hockemeyer, D., Ngai, J., & Bateup, H. S. (2021). Generation of a DAT-Flp mouse line for intersectional genetic targeting of dopamine neuron subpopulations. *Cell Reports*, *35*(6). https://doi.org/10.1101/2020.06.24.167908

Kuo, H. Y., & Liu, F. C. (2020). Pathological alterations in striatal compartments in the human brain of autism spectrum disorder. *Molecular Brain*, *13*(1), 2–5. https://doi.org/10.1186/s13041-020-00624-2

Lammel, S., Steinberg, E. E., Földy, C., Wall, N. R., Beier, K., Luo, L., & Malenka, R. C. (2015). Diversity of transgenic mouse models for selective targeting of midbrain dopamine neurons. *Neuron*, *85*(2), 429–438. https://doi.org/10.1016/j.neuron.2014.12.036

Langen, M., Schnack, H. G., Nederveen, H., Bos, D., Lahuis, B. E., de Jonge, M. V., van Engeland, H., & Durston, S. (2009). Changes in the Developmental Trajectories of Striatum in Autism. *Biological Psychiatry*, *66*(4), 327–333. https://doi.org/10.1016/j.biopsych.2009.03.017

Leroux-Nicollet, I., Darchen, F., Scherman, D., & Costentin, J. (1990). Postnatal development of the monoamine vesicular transporter in mesencephalic and telencephalic regions of the rat brain: A quantitative autoradiographic study with [3H]dihydrotetrabenazine. *Neuroscience Letters*, *117*(1–2), 1–7. https://doi.org/10.1016/0304-3940(90)90110-U

Lieberman, O. J., McGuirt, A. F., Mosharov, E. V., Pigulevskiy, I., Hobson, B. D., Choi, S., Frier, M. D., Santini, E., Borgkvist, A., & Sulzer, D. (2018). Dopamine Triggers the Maturation of Striatal Spiny Projection Neuron Excitability during a Critical Period. *Neuron*, *99*(3), 540-554.e4. https://doi.org/10.1016/J.NEURON.2018.06.044

Liu, C., & Kaeser, P. S. (2019). Mechanisms and regulation of dopamine release. *Current Opinion in Neurobiology*, *57,* 46–53. https://doi.org/10.1016/j.conb.2019.01.001

Liu, C., Kershberg, L., Wang, J., Schneeberger, S., & Kaeser, P. S. (2018). Dopamine Secretion Is Mediated by Sparse Active Zone-like Release Sites. *Cell*, *172*(4), 706-718.e15. https://doi.org/10.1016/j.cell.2018.01.008

Maenner, M. J., Shaw, K. A., Baio, J., Washington, A., Patrick, M., DiRienzo, M., Christensen, D. L., Wiggins, L. D., Pettygrove, S., Andrews, J. G., Lopez, M., Hudson, A., Baroud, T., Schwenk, Y., White, T., Rosenberg, C. R., Lee, L. C., Harrington, R. A., Huston, M., … Dietz, P. M. (2020). Prevalence of Autism Spectrum Disorder Among Children Aged 8 Years - Autism and Developmental Disabilities Monitoring Network, 11 Sites, United States, 2016. *Morbidity and Mortality Weekly Report. Surveillance Summaries (Washington, D.C. : 2002)*, *69*(4), 1–12. https://doi.org/10.15585/MMWR.SS6904A1

Märtin, A., Calvigioni, D., Tzortzi, O., Fuzik, J., Wärnberg, E., & Meletis, K. (2019). A Spatiomolecular Map of the Striatum. *Cell Reports*, *29*(13), 4320-4333.e5. https://doi.org/10.1016/J.CELREP.2019.11.096

Mathis, A., Mamidanna, P., Cury, K. M., Abe, T., Murthy, V. N., Mathis, M. W., & Bethge, M. (2018). DeepLabCut: markerless pose estimation of user-defined body parts with deep learning. *Nature Neuroscience*, *21*(9), 1281–1289. https://doi.org/10.1038/s41593-018-0209-y

Matsuda, W., Furuta, T., Nakamura, K. C., Hioki, H., Fujiyama, F., Arai, R., & Kaneko, T. (2009). Single nigrostriatal dopaminergic neurons form widely spread and highly dense axonal arborizations in the neostriatum. *The Journal of Neuroscience*, *29*(2), 444–453. https://doi.org/10.1523/JNEUROSCI.4029-08.2009

Matsushima, A., & Graybiel, A. M. (2020). Combinatorial Developmental Controls on Striatonigral Circuits. *Cell Reports*, *31*(11). https://doi.org/10.1016/J.CELREP.2020.107778

Mingote, S., Amsellem, A., Kempf, A., Rayport, S., & Chuhma, N. (2019). Dopamine-glutamate neuron projections to the nucleus accumbens medial shell and behavioral switching. *Neurochemistry International*, *129*. https://doi.org/10.1016/j.neuint.2019.104482

Modi, M. E., & Sahin, M. (2019). A unified circuit for social behavior. *Neurobiology of Learning and Memory*, *165*. https://doi.org/10.1016/j.nlm.2018.08.010

Morigaki, R., & Goto, S. (2016). Putaminal mosaic visualized by tyrosine hydroxylase immunohistochemistry in the human neostriatum. *Frontiers in Neuroanatomy*, *10*(APR), 1–12. https://doi.org/10.3389/fnana.2016.00034

Nakamura, K., Hioki, H., Fujiyama, F., & Kaneko, T. (2005). Postnatal changes of vesicular glutamate transporter (VGluT)1 and VGluT2 immunoreactivities and their colocalization in the mouse forebrain. *Journal of Comparative Neurology*, *492*(3), 263–288. https://doi.org/10.1002/CNE.20705

Nectow, A. R., & Nestler, E. J. (2020). Viral tools for neuroscience. *Nature Reviews Neuroscience*, *21*(12), 669–681. https://doi.org/10.1038/s41583-020-00382-z

Neniskyte, U., & Gross, C. T. (2017). Errant gardeners: glial-cell-dependent synaptic pruning and neurodevelopmental disorders. *Nature Reviews Neuroscience*, *18*(11), 658–670. https://doi.org/10.1038/nrn.2017.110

Niederkofler, V., Asher, T. E., Okaty, B. W., Rood, B. D., Narayan, A., Hwa, L. S., Beck, S. G., Miczek, K. A., & Dymecki, S. M. (2016). Identification of Serotonergic Neuronal Modules that Affect Aggressive Behavior. *Cell Reports*, *17*(8), 1934–1949. https://doi.org/10.1016/j.celrep.2016.10.063

Ozonoff, S., Iosif, A.-M., Baguio, F., Cook, I. C., Hill, M. M., Hutman, T., Rogers, S. J., Rozga, A., Sangha, S., Sigman, M., Steinfeld, M. B., & Young, G. S. (2010). A Prospective Study of the Emergence of Early Behavioral Signs of Autism. *Journal of the American Academy of Child & Adolescent Psychiatry*, *49*(3), 256-266.e2. https://doi.org/10.1016/J.JAAC.2009.11.009

Pavăl, D. (2017). A Dopamine Hypothesis of Autism Spectrum Disorder. *Developmental Neuroscience*, *39*(5), 355–360. https://doi.org/10.1159/000478725

Peça, J., Feliciano, C., Ting, J. T., Wang, W., Wells, M. F., Venkatraman, T. N., Lascola, C. D., Fu, Z., & Feng, G. (2011). Shank3 mutant mice display autistic-like behaviours and striatal dysfunction. *Nature*, *472*(7344), 437–442. https://doi.org/10.1038/nature09965

Peixoto, R. T., Chantranupong, L., Hakim, R., Levasseur, J., Wang, W., Merchant, T., Gorman, K., Budnik, B., & Sabatini, B. L. (2019). Abnormal Striatal Development Underlies the Early Onset of Behavioral Deficits in Shank3B−/− Mice. *Cell Reports*, *29*(7), 2016-2027.e4. https://doi.org/10.1016/j.celrep.2019.10.021

Phelan, K., & McDermid, H. E. (2012). The 22q13.3 deletion syndrome (Phelan-McDermid syndrome). *Molecular Syndromology*, *2*(3–5), 186–201. https://doi.org/10.1159/000334260

Poulin, J.-F., Gaertner, Z., Moreno-Ramos, O. A., & Awatramani, R. (2020). Classification of Midbrain Dopamine Neurons Using Single-Cell Gene Expression Profiling Approaches. *Trends in Neurosciences*, *43*(3), 155–169. https://doi.org/10.1016/j.tins.2020.01.004

Poulin, J. F., Caronia, G., Hofer, C., Cui, Q., Helm, B., Ramakrishnan, C., Chan, C. S., Dombeck, D. A., Deisseroth, K., & Awatramani, R. (2018). Mapping projections of molecularly defined dopamine neuron subtypes using intersectional genetic approaches. *Nature Neuroscience*, *21*(9), 1260–1271. https://doi.org/10.1038/s41593-018-0203-4

Quesnel-Vallières, M., Weatheritt, R. J., Cordes, S. P., & Blencowe, B. J. (2018). Autism spectrum disorder: insights into convergent mechanisms from transcriptomics. *Nature Reviews Genetics*, *20*(1), 51–63. https://doi.org/10.1038/s41576-018-0066-2

Rein, B., Ma, K., & Yan, Z. (2020). A standardized social preference protocol for measuring social deficits in mouse models of autism. *Nature Protocols*, *15,* 3464-3477. https://doi.org/10.1038/s41596-020-0382-9

Reynolds, L. M., & Flores, C. (2021). Mesocorticolimbic Dopamine Pathways Across Adolescence: Diversity in Development. *Frontiers in Neural Circuits*, *15*, 94. https://doi.org/10.3389/FNCIR.2021.735625/BIBTEX

Salgado, S., & Kaplitt, M. G. (2015). The Nucleus Accumbens: A Comprehensive Review. *Stereotactic and Functional Neurosurgery*, *93*(2), 75–93. https://doi.org/10.1159/000368279

Schultz, W. (2017). Reward prediction error. *Current Biology*, *27*(10), R369–R371. https://doi.org/10.1016/J.CUB.2017.02.064

Scott-Van Zeeland, A. A., Dapretto, M., Ghahremani, D. G., Poldrack, R. A., & Bookheimer, S. Y. (2010). Reward processing in autism. *Autism Research*, *3*(2), 53–67. https://doi.org/10.1002/AUR.122

Silverman, J. L., Yang, M., Lord, C., & Crawley, J. N. (2010). Behavioural phenotyping assays for mouse models of autism. *Nature Reviews Neuroscience*, *11*(7), 490–502. https://doi.org/10.1038/nrn2851

Sparks, B. F., Friedman, S. D., Shaw, D. W., Aylward, E. H., Echelard, D., Artru, A. A., Maravilla, K. R., Giedd, J. N., Munson, J., Dawson, G., & Dager, S. R. (2002). Brain structural abnormalities in young children with autism spectrum disorder. *Neurology*, *59*(2), 184–192. https://doi.org/10.1212/WNL.59.2.184

Sulzer, D., Joyce, M. P., Lin, L., Geldwert, D., Haber, S. N., Hattori, T., & Rayport, S. (1998). Dopamine neurons make glutamatergic synapses in vitro. *The Journal of Neuroscience*, *18*(12), 4588–4602. https://doi.org/10.1523/JNEUROSCI.18-12-04588.1998

Tang, G., Gudsnuk, K., Kuo, S. H., Cotrina, M. L., Rosoklija, G., Sosunov, A., Sonders, M. S., Kanter, E., Castagna, C., Yamamoto, A., Yue, Z., Arancio, O., Peterson, B. S., Champagne, F., Dwork, A. J., Goldman, J., & Sulzer, D. (2014). Loss of mTOR-Dependent Macroautophagy Causes Autistic-like Synaptic Pruning Deficits. *Neuron*, *83*(5), 1131–1143. https://doi.org/10.1016/J.NEURON.2014.07.040

Tepper, J. M., & Trent, F. (1993). In vivo studies of the postnatal development of rat neostriatal neurons. *Progress in Brain Research*, *99*(C), 35–50. https://doi.org/10.1016/S0079-6123(08)61337-0

Valtorta, F., Pennuto, M., Bonanomi, D., & Benfenati, F. (2004). Synaptophysin: leading actor or walk-on role in synaptic vesicle exocytosis? *BioEssays*, *26*(4), 445–453. https://doi.org/10.1002/BIES.20012

Vizi, E., Fekete, A., Karoly, R., & Mike, A. (2010). Non-synaptic receptors and transporters involved in brain functions and targets of drug treatment. *British Journal of Pharmacology*, *160*, 785–809. https://doi.org/doi:10.1111/j.1476-5381.2009.00624.x

Voorn, P., Kalsbeek, A., Jorritsma-Byham, B., & Groenewegen, H. J. (The pre- and postnatal development of the dopaminergic cell groups in the ventral mesencephalon and the dopaminergic innervation of the striatum of the rat. *Neuroscience*, *25*(3), 857–887. https://doi.org/10.1016/0306-4522(88)90041-3

Watabe-Uchida, M., Zhu, L., Ogawa, S. K., Vamanrao, A., & Uchida, N. (2012). Whole-brain mapping of direct inputs to midbrain dopamine neurons. *Neuron*, *74*(5), 858–873. https://doi.org/10.1016/J.NEURON.2012.03.017

Weihe, E., Depboylu, C., Schuẗz, B., Schäfer, M. K. H., & Eiden, L. E. (2006). Three Types of Tyrosine Hydroxylase-Positive CNS Neurons Distinguished by Dopa Decarboxylase and VMAT2 Co-Expression. *Cellular and Molecular Neurobiology*, *26*, 657-676. https://doi.org/10.1007/S10571-006-9053-9

Wolterink-Donselaar, I. G., Meerding, J. M., & Fernandes, C. (2009). A method for gender determination in newborn dark pigmented mice. *Lab Animal*, *38*(1), 35–38. https://doi.org/10.1038/laban0109-35

Wright, J., Stanic, D., & Thompson, L. H. (2013). Generation of striatal projection neurons extends into the neonatal period in the rat brain. *The Journal of Physiology*, *591*(1), 67-76. https://doi.org/10.1113/JPHYSIOL.2012.246397

Xenias, H. S., Ibáñez-Sandoval, O., Koós, T., & Tepper, J. M. (2015). Are Striatal Tyrosine Hydroxylase Interneurons Dopaminergic? *The Journal of Neuroscience*, *35*(16), 6584. https://doi.org/10.1523/JNEUROSCI.0195-15.2015

Zhang, S., Qi, J., Li, X., Wang, H. L., Britt, J. P., Hoffman, A. F., Bonci, A., Lupica, C. R., & Morales, M. (2015). Dopaminergic and glutamatergic microdomains in a subset of rodent mesoaccumbens axons. *Nature Neuroscience*, *18*(3), 386–392. https://doi.org/10.1038/nn.3945

Zhao, H., Tu, Z., Xu, H., Yan, S., Yan, H., Zheng, Y., Yang, W., Zheng, J., Li, Z., Tian, R., Lu, Y., Guo, X., Jiang, Y. H., Li, X. J., & Zhang, Y. Q. (2017). Altered neurogenesis and disrupted expression of synaptic proteins in prefrontal cortex of SHANK3-deficient non-human primate. *Cell Research*, *27*(10), 1293–1297. https://doi.org/10.1038/cr.2017.95

Zhou, Y., Sharma, J., Ke, Q., Landman, R., Yuan, J., Chen, H., Hayden, D. S., Fisher, J. W., Jiang, M., Menegas, W., Aida, T., Yan, T., Zou, Y., Xu, D., Parmar, S., Hyman, J. B., Fanucci-Kiss, A., Meisner, O., Wang, D., … Yang, S. (2019). Atypical behaviour and connectivity in SHANK3-mutant macaques. *Nature*, *570*(7761), 326–331. https://doi.org/10.1038/s41586-019-1278-0

Zürcher, N. R., Walsh, E. C., Phillips, R. D., Cernasov, P. M., Tseng, C. E. J., Dharanikota, A., Smith, E., Li, Z., Kinard, J. L., Bizzell, J. C., Greene, R. K., Dillon, D., Pizzagalli, D. A., Izquierdo-Garcia, D., Truong, K., Lalush, D., Hooker, J. M., & Dichter, G. S. (2021). A simultaneous [11C]raclopride positron emission tomography and functional magnetic resonance imaging investigation of striatal dopamine binding in autism. *Translational Psychiatry*, *11*(33). https://doi.org/10.1038/s41398-020-01170-0